

## Article

# Assessment of Groundwater Potential Zones Utilizing Geographic Information System-Based Analytical Hierarchy Process, Vlse Kriterijumska Optimizacija Kompromisno Resenje, and Technique for Order Preference by Similarity to Ideal Solution Methods: A Case Study in Mersin, Türkiye

Mehmet Özgür Çelik \*, Lütfiye Kuşak  and Murat Yakar 

Geomatics Engineering Department, Engineering Faculty, Mersin University, 33343 Mersin, Türkiye; lutfiyekusak@mersin.edu.tr (L.K.); myakar@mersin.edu.tr (M.Y.)

\* Correspondence: mozgurcelik33@gmail.com

**Abstract:** The indiscriminate use of surface water has heightened the demand for groundwater supplies. Therefore, it is critical to locate potential groundwater sources to develop alternative water resources. Groundwater detection is tremendously valuable, as is sustainable groundwater management. Mersin, in southern Türkiye, is expected to confront drought shortly due to increased population, industry, and global climate change. The groundwater potential zones of Mersin were determined in this study by GIS-based AHP, VIKOR, and TOPSIS methods. Fifteen parameters were used for this goal. The study area was separated into five categories. The results show that the study area can be divided into “Very High” zones (4.98%, 5.94%, 7.96%), followed by “High” zones (10.89%, 10.32%, 16.50%), “Moderate” zones (60.68%, 52.41%, 51.56%), “Low” zones (21.28%, 28.53%, 20.90%), and “Very Low” zones (2.18%, 2.80%, 3.07%) in turn. Data from 60 wells were used to validate potential groundwater resources. The ROC-AUC technique was utilized for this. It was seen that the performance of the VIKOR model is better than that of the AHP and TOPSIS (76.5%). The findings demonstrated that the methods and parameters used are reliable for sustainable groundwater management. We believe that the study will also help decision makers for this purpose.

**Keywords:** AHP; GIS; groundwater potential zone; sustainable groundwater management; TOPSIS; VIKOR



**Citation:** Çelik, M.Ö.; Kuşak, L.; Yakar, M. Assessment of Groundwater Potential Zones Utilizing Geographic Information System-Based Analytical Hierarchy Process, Vlse Kriterijumska Optimizacija Kompromisno Resenje, and Technique for Order Preference by Similarity to Ideal Solution Methods: A Case Study in Mersin, Türkiye. *Sustainability* **2024**, *16*, 2202. <https://doi.org/10.3390/su16052202>

Academic Editors: Johnbosco C. Egbueri, Peiyue Li and Antonije Onjia

Received: 16 February 2024

Revised: 1 March 2024

Accepted: 3 March 2024

Published: 6 March 2024



**Copyright:** © 2024 by the authors. Licensee MDPI, Basel, Switzerland. This article is an open access article distributed under the terms and conditions of the Creative Commons Attribution (CC BY) license (<https://creativecommons.org/licenses/by/4.0/>).

## 1. Introduction

Water is the most fundamental source of life for all living things. It is well known that from the past to the present, the overuse of water, a scarce and restricted resource, has caused a decline in surface water [1]. During excessive and uncontrolled use, organic and heavy metal pollution have accumulated in surface waters and caused the quality of the water to decrease [2,3]. At the same time, global issues such as climate change and drought have severely impacted or even destroyed surface water [4]. For all of these reasons, the demand for groundwater has increased [5]. Groundwater is the leading freshwater resource for domestic and agricultural use [6,7]. Groundwater is the principal water resource for agriculture, industry, and domestic uses, particularly in drylands where annual rainfall is low [8]. Agricultural activities use 42% of the total groundwater worldwide [9]. Groundwater accounts for approximately 50% of irrigation activities in India, one of the world’s largest water consumers. In China, groundwater is used to irrigate around 9 million hectares (ha) of land [10]. The Ogallala and High Plains Aquifers, two of the major groundwater aquifers in the United States, are extensively exploited for irrigation. Groundwater constitutes approximately 23% of the total water resources in the United States, with 68.4% being used for irrigation [8].

However, in Türkiye, agriculture uses 77% of the 58.95 billion cubic meters of water, while drinking water and industries consume 23% [11].

Groundwater is a dynamic and renewable natural resource that provides consistent economic growth and drinking water in urban and rural areas [12]. In this setting, investigations to determine existing groundwater assets and potential zones are of critical importance [13]. However, detecting groundwater is more complicated than recognizing surface water. There are standard and dependable methods for determining groundwater and other ground information, such as test drilling and stratigraphic analysis [7]. However, the methods described are costly, time-consuming, and rely on human resources [14]. The methods utilized today include the analytical hierarchy process (AHP), Vlse Kriterijska Optimizacija Kompromisno Resenje (VIKOR), and the Technique for Order Preference by Similarity to Ideal Solution (TOPSIS), which are based on the geographic information system (GIS) technique [15–27].

Different parameters are preferred in the various methods used to determine potential groundwater resources, and activities are conducted accordingly. Hence, the parameters employed in determining groundwater potential resources are essential. Land use/land cover (LuLc), soil, geology, slope, lineament, drainage density, TWI, SPI, and STI are parameters frequently used for this purpose [28,29]. However, depending on the study area, the parameters utilized to identify potential groundwater may differ (Table 1).

**Table 1.** Literature review of the parameters used to determine a groundwater potential zone (GWPZ).

Reference	Parameters														
	G	GM	LI	S	SL	RF	DD	LD	LuLc	WTD	RR	TWI	SW	DEM	VC
[30]	•	•		•	•		•	•	•		•				
[31]	•	•		•	•	•		•	•	•				•	•
[32]	•				•	•	•	•						•	
[33]	•	•			•	•	•	•						•	
[34]	•	•		•	•	•	•	•	•			•			
[35]				•	•	•			•					•	
[12]	•	•		•	•	•			•	•				•	
[36]	•	•		•	•	•	•	•	•						
[37]	•	•		•	•	•	•	•	•						
[38]		•	•	•	•		•	•	•						
[39]		•	•		•		•	•							
[40]		•	•	•	•	•	•	•	•						
[41]		•	•	•	•		•	•	•						

G = geology; GM = geomorphology; LI = lithology; S = soil texture; SL = slope; RF = rainfall; DD = drainage density; LD = lineament density; LuLc = land use/land cover; WTD = water table depth; RR = recharge rate; TWI = topographic wetness index; SW = surface water body; DEM = digital elevation model; VC = vegetation cover.

Groundwater is critically important, especially in arid or drought-prone areas, and must be managed as effectively as possible once determined. Mersin is threatened by aridity due to its geography, drought, and global climate change. Groundwater is extremely vital for Mersin, which is located in the Mediterranean basin, which is a semi-arid climate zone. Mersin is also a significant city in Türkiye, whose agricultural activity takes up around 20.91% of its surface area [42]. Surface water and groundwater are both known to be employed in agricultural activities, and these activities strain the limited resources of water. The increasing population also exacerbates the current unfavorable situation. These are the reasons why it was selected as the study area and the application was generated here.

The potential groundwater detection zone of Mersin was determined using the GIS-based AHP, VIKOR, and TOPSIS methods with fifteen parameters. Water resources, rainfall, irrigated farming areas, plains, lineament density, geology, slope, soil, land use/land cover (LuLc), drainage density, water erosion, topographic wetness index (TWI), topographic roughness index (TRI), stream power index (SPI), and sediment transport index (STI) are

the parameters (Table 2). This study was conducted due to the absence of a large-scale investigation to define the GWPZ of Mersin. Furthermore, the location of Mersin and its characteristics made it the subject of this investigation. All the same, the study is important for sustainable groundwater management.

**Table 2.** The parameters used to determine groundwater potential zones (GWPZs).

Parameters	Scale/Resolution → Final Resolution	Data Type	Source
Water resources	1:100,000 → 30 m	Vector	RTMAF [43]
Rainfall	30 arc second → 30 m	Raster	WorldClim [44]
Irrigated farming areas	1:100,000 → 30 m	Vector	RTMAF [43]
Plains	1:100,000 → 30 m	Vector	RTMEUCC [45]
Lineament density	30 m	Raster	Production
Geology	1/100,000 → 30 m	Vector	USGS [46]
Slope	30 m	Raster	Production from DEM
Soil	1/100,000 → 30 m	Raster	RTGDMRE [45]
LuLc	1/100,000 → 30 m	Raster	CLMS [47]
Drainage density	30 m	Raster	Production
Water erosion	1:100,000 → 30 m	Vector	RTMAF [43]
TWI	30 m	Raster	Production
TRI	30 m	Raster	Production
SPI	30 m	Raster	Production
STI	30 m	Raster	Production

CLMS: Copernicus Land Monitoring Service; USGS: United States Geological Survey; RTMAF: Republic of Türkiye Ministry of Agriculture and Forestry; RTGDMRE: Republic of Türkiye General Directorate of Mineral Research and Exploration; RTMEUCC: Republic of Türkiye Ministry of Environment, Urbanization, and Climate Change.

## 2. Study Area

The study area is Mersin, which is located in southern Türkiye between 36 and 37° North latitudes and 33 and 35° East longitudes, where the Mediterranean climate prevails (Figure 1). It covers 15,853 km<sup>2</sup> and has a population of roughly 2 million [48].

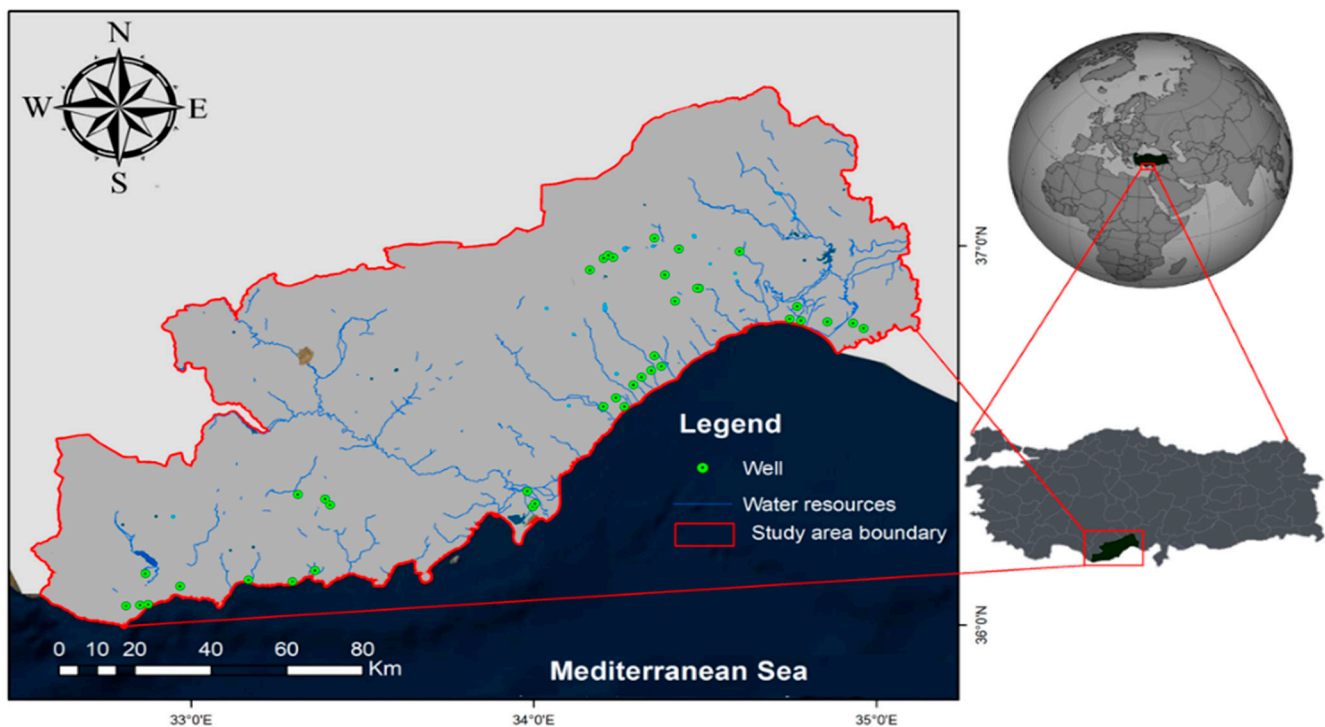


**Figure 1.** Study area.

Given that Mersin is a coastal city, the altitude in the city center and coastal district ranges between 0 and 10 m. The altitude reached 3500 m in the Taurus Mountains, the highest point in Mersin. Aside from coastal areas, mountainous regions are widespread in the study area [49]. Although the area's land surface varies, it is composed of limestone, sandstone, alluvium, and dolomite. Animal husbandry is the principal source of income in hilly places with steep slopes, and active agriculture takes place in the plains and low-sloped areas. Mersin is a significant city in Türkiye, whose agricultural activity takes up around 20.91% of its surface area [42]. The annual temperature is 27.1 °C in the summer period (June, July, and August) and 11.1 °C in the winter months (December, January, and February) (General Directorate of Meteorology, 2023). The annual average rainfall is 28.8 mm in the summer period and 344.3 mm in the winter months with the highest precipitation, and the annual average rainfall is 613.2 mm [50]. The world average is 900 mm [51].

Mersin has been more urbanized as a result of rapid population growth, particularly in the fifteen years preceding this one. Water use increases as the population grows, putting pressure on the resource. Mersin, like the rest of Türkiye, is suffering from water scarcity. Mersin was chosen as the study area based on its aforementioned features.

### 3. Materials and Methods

The methodology for the study is to determine the GWPZ using fifteen criteria. Three different GIS-based methodologies (AHP, VIKOR, TOPSIS) were chosen for this purpose (Figure 2). The AHP, VIKOR, and TOPSIS methods were applied sequentially. Firstly, the parameters were defined. GWPZ detection is extremely important due to the location and characteristics of the study area. The resolution of the parameters employed has a direct impact on the accuracy of the detection process. For all these reasons, high-resolution parameters were opted for, and analyses were conducted. Secondly, models were constructed using the methods in ArcGIS 10.5 software, and finally, an accuracy analysis of the created models was evaluated with the ArcSDM tool in ArcGIS.

#### 3.1. Definition of the Thematic Layers

##### 3.1.1. Topographical Data

###### Soil

The soil layer is the most significant and primary layer for the percolation of water [52]. The water penetration rate beneath the soil is proportional to the soil's permeability and water-holding capacity [53]. Therefore, it affects GWPZ detection investigations [31]. The soil map was organized into eight classes (Figure 3a). The study occurred, respectively, on 6.28% alluvial soil, 0.48% beach sand, dunes, and marsh soil, 0.28% halomorphic soil, 0.52% hydromorphic saline soil, 75.64% red podzolic soil, 4.95% terra rose soil, 1.24% terra rose soil moderately sloping, and 10.61% volcanic and igneous rocks soil. Because of their high water-holding capacity and clay content, alluvial and hydromorphic saline soil types received the highest score of five. One point was given because detecting groundwater in podzolic soils is challenging [7].

###### Geology

Groundwater formation and movement are influenced by many geological formations. Besides that, geological formations play a role in determining GWPZs [34]. The geology map was taken from USGS, and it was digitized. Sixteen classes were determined in total (Figure 3b). In the middle of the study area, Neogene formations are common. It covers 9130 km<sup>2</sup> (56.7%). In the west of the study area, the Precambrian–Paleozoic formations cover 468 km<sup>2</sup> (2.91%). This is critical for a GWPZ owing to its clayey structure. A value of four was given to it. Sea and large lake formations are the most important for indicating water potential, and they cover 25 km<sup>2</sup> (0.15%). Hence, a value of five was assigned to it. Another essential type of formation are undivided quaternary formations. They are predominantly in the south of the study area and cover 1219 km<sup>2</sup> (7.6%).

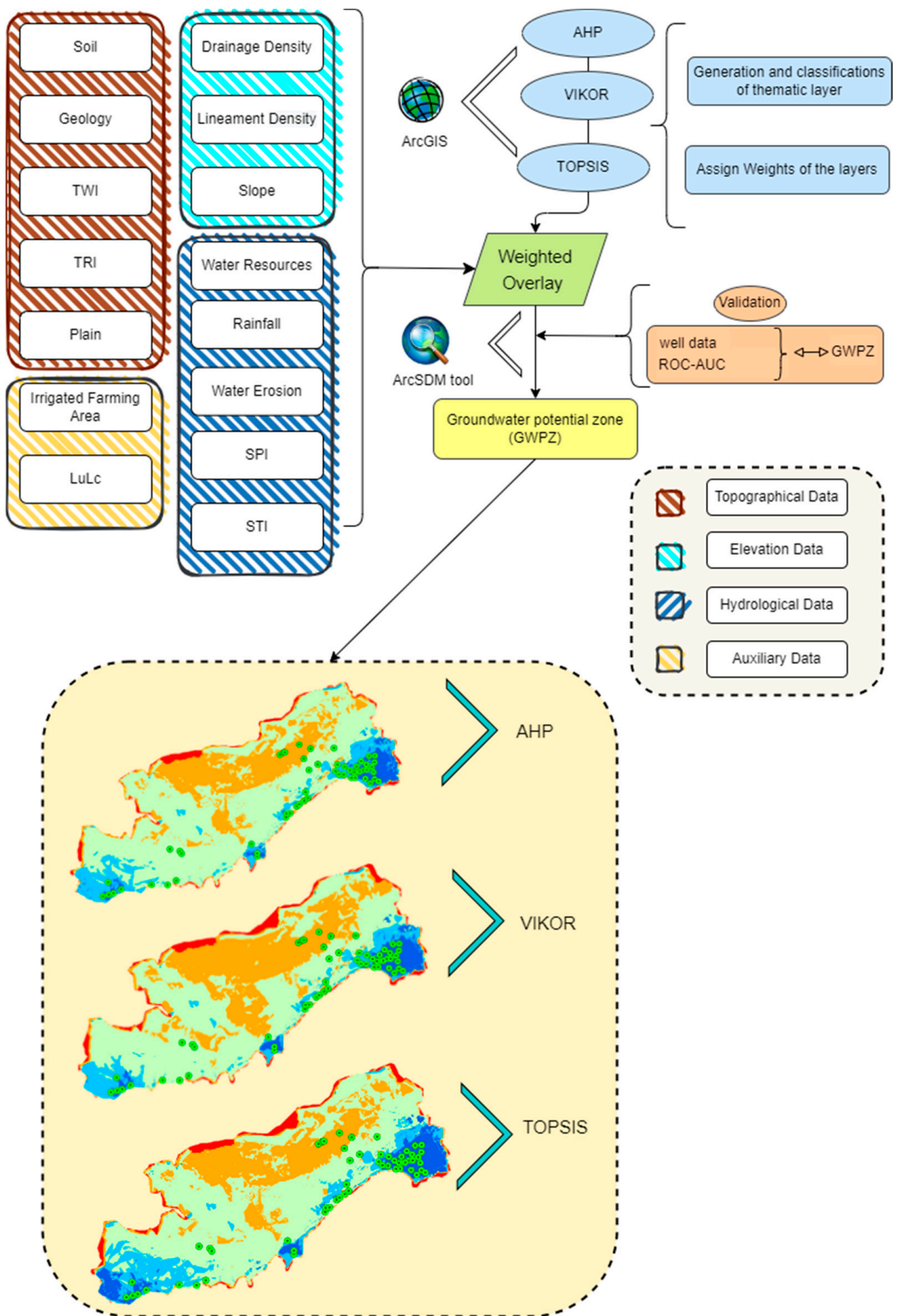


Figure 2. Flow chart of the methodology.

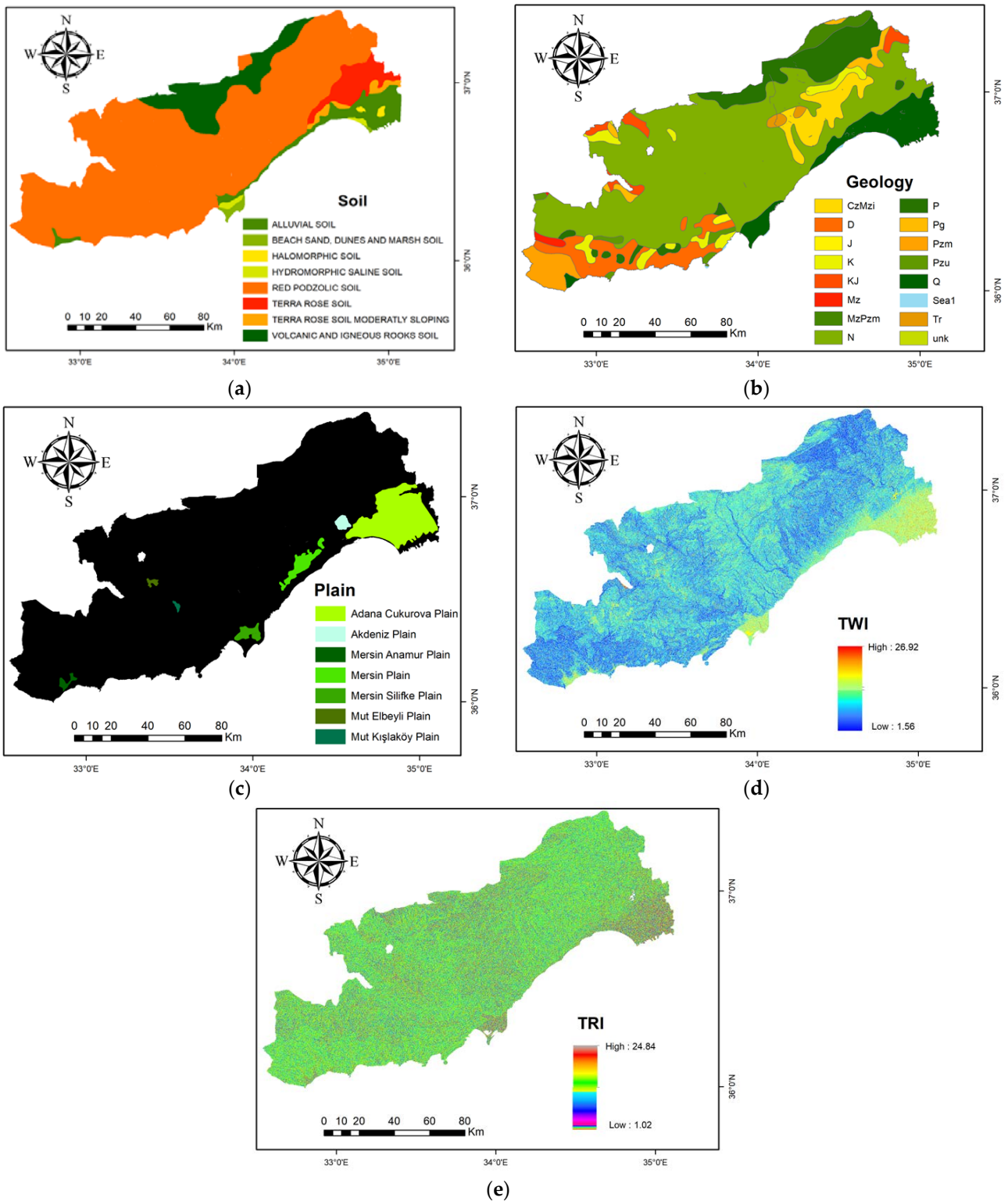


Figure 3. (a) Soil, (b) geology, (c) TWI, (d) TRI, and (e) plains.

Topographic Wetness Index (TWI)

The TWI is essential in hydrological processes and flows [54]. It contributes to uncovering dependable knowledge about flow formation and inflow. Accordingly, it is a significant parameter in determining GWPZs. A high TWI supports a strong possibility of

groundwater [55]. The TWI is calculated using Equation (1). The TWI map was created with ArcGIS software using hydrology tools (Figure 3d).

$$TWI = A_s / \tan\beta \quad (1)$$

where  $A_s$  is the cumulative area or flow accumulation and  $\beta$  represents the slope gradient.

#### Topographic Roughness Index (TRI)

The TRI is another parameter used effectively in GWPZ analyses [56]. It is also a geomorphological parameter that affects the spatial distribution and number of hills and valleys in the study area. The TRI affects groundwater potential. It plays a significant role in the analysis, like the TWI. The TRI was calculated using Equation (2) (Figure 3e).

$$TRI = \sqrt{\left| \left( \max^2 - \min^2 \right) \right|} \quad (2)$$

where  $\max$  and  $\min$  reflect the largest and smallest values of the height of each pixel.

#### Plains

There are many plains in Türkiye. The study area is 8.1% plains. Plains tend to have fertile soils and abundant water resources. Plains are particularly well known for their proximity to groundwater resources. The plain layer was downloaded to the ATLAS application and digitized (Figure 3c). A single class was generated for the layer.

#### 3.1.2. Elevation Data

##### Drainage Density

The drainage density is inversely proportional to the permeability, which affects the inflow [57]. A low drainage density is a decisive parameter for more leakage [58]. In other words, it is inversely related to lineament density. The drainage density map was generated using the DEM with several spatial analyses (Equation (3)). The data were classified into five categories (Figure 4a).

$$DD = \sum_{i=1}^n D_i / A \quad (3)$$

where  $D_i$  is the length of streams and  $A$  is the water area.

##### Lineament Density

Lineaments are parameters that indicate potential water resources and provide a pathway for water [59]. The lineament density points out a permeant region [60]. Hence, it plays a substantial role in determining GWPZs. The lineaments were construed with the DEM. The Hillshade layer, which has different angular values, was created utilizing the DEM. The layer was digitized, and the lineament density was produced using Equation (4). The lineament density was organized into five classes on ArcGIS software with a density process (Figure 4b).

$$LD = \sum_{i=1}^n L_i / A \quad (4)$$

where  $L_i$  represents the length of the  $i$ th lineament and  $A$  is the area.

##### Slope

Aside from determining GWPZs, the slope provides information on the surface water-holding capacity [61]. It affects the rainfall rate and runoff accumulation [62]. Low-slope regions tend to have high groundwater potential. The slope map was created utilizing the DEM (Figure 4c). The slope data were grouped into five classes: 0–5.12°, very high potential; 5.12–11.53°, high potential; 11.53–18.59°, good potential; 18.59–26.60°, moderate potential; 26.60–36.86°, low potential; and 36.86–81.74°, very low potential. These different slope

potentials made up, respectively, 7.01% (1125 km<sup>2</sup>), 6.34% (1019 km<sup>2</sup>), 6% (963 km<sup>2</sup>), 0.34% (55 km<sup>2</sup>), 9.19% (1474 km<sup>2</sup>), 2.80% (450 km<sup>2</sup>), and 68.32% (10,969 km<sup>2</sup>) of the study area.

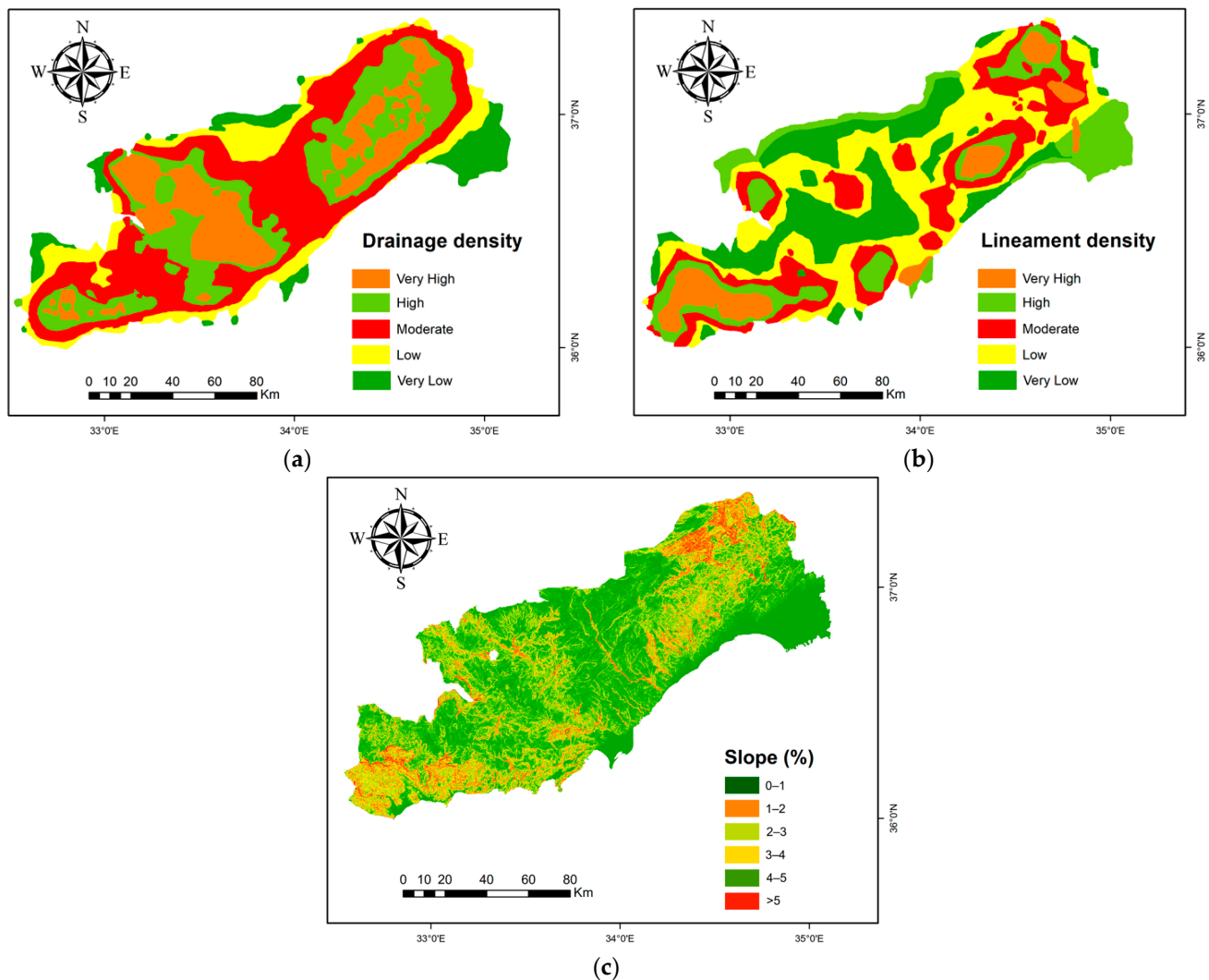


**Figure 4.** (a) Drainage density, (b) lineament density, (c) slope.

### 3.1.3. Hydrological Data

#### Water Resources

Streams, rivers, water bodies, canals, dams, lakes, and ponds are water resources in the study area. Water resources play a significant part in groundwater recharge [31]. They also indicate the potential presence of groundwater. It is essential to determine the current groundwater level and how it is controlled [63]. The water resources in the study area were obtained from TadPortal, digitized, and organized into seven classes (Figure 5a).

#### Rainfall

The annual average rainfall is used to determine potential groundwater regions and is a significant parameter for this goal. Regions with low annual average rainfall are prone to low groundwater potential. Mersin province rainfall data were obtained from WorldClim, and Mersin's rainfall showed a change of 450–950 mm when the rainfall data were examined. It was especially noted that Anamur and southern Tarsus had the highest levels of rainfall. The rainfall map was created in Mersin, which has an annual average amount of rainfall of 613 mm. The map was organized into four classes (Figure 5b).

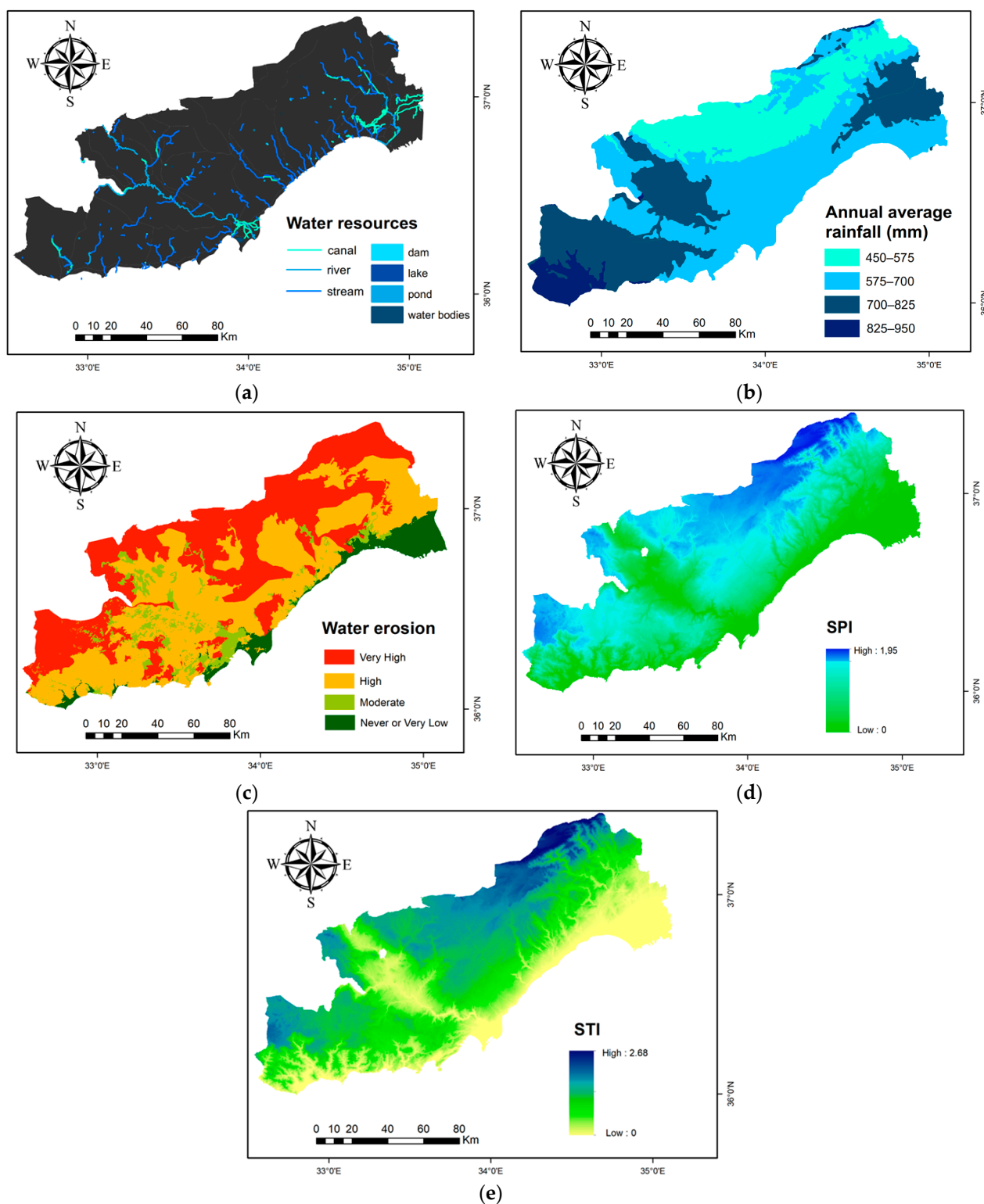


**Figure 5.** (a) Water resources, (b) rainfall, (c) water erosion, (d) SPI, and (e) STI.

### Water Erosion

The process by which rainwater that cannot be absorbed by the soil is carried to another place by a slope is called water erosion. There is a close relationship between heavy rainfall and water erosion [64]. In addition, water erosion shows an alteration in soil type, permeability, and land characteristics [65]. It is crucial in groundwater analysis. The water

erosion data in the study were digitized from TadPortal with great effort, and the data were grouped into four classes (Figure 5c).

#### Stream Power Index (SPI)

The SPI is a parameter that is determined by the abrasive power of water and sediment and the water-bearing capacity and is therefore related to water erosion [66]. The SPI is a significant parameter for determining GWPZs [67]. The SPI in the study was calculated using Equation (5). The SPI map was generated (Figure 5d).

$$SPI = A_s \tan \beta \quad (5)$$

#### Sediment Transport Index (STI)

The STI is a parameter used to survey the water-bearing capacity as it varies with slope [68]. The STI is directly proportional to the abrasive power of water, as is the SPI. The STI was computed using Equation (6). The STI map was created the same way as for the other parameters (Figure 5e).

$$STI = (A_s / 22.13)^{0.6} (\sin \beta / 0.0896)^{1.3} \quad (6)$$

where  $A_s$  is the cumulative area, and  $\beta$  is the slope gradient in Equations (5) and (6).

#### 3.1.4. Auxiliary Data

##### Irrigated Farming Areas

Surface water or groundwater is generally utilized in irrigated farming areas [69]. The irrigation application uses approximately 45.05 billion cubic meters of water in Türkiye [11], and it is thought that this will increase in the future. It is known that groundwater is commonly used in agricultural activities these days [70]. Agricultural activities are executed in nearly a quarter of the study area, and irrigated farming activities particularly stress water. Determining groundwater as an alternative water resource is vital to preventing the disruption of agricultural activities. The irrigated farming area layer was obtained from TadPortal and digitized. A single class was constructed, like for the plains layer (Figure 6a). This parameter was used for control purposes rather than determining groundwater potential zones since there is water use in these areas.

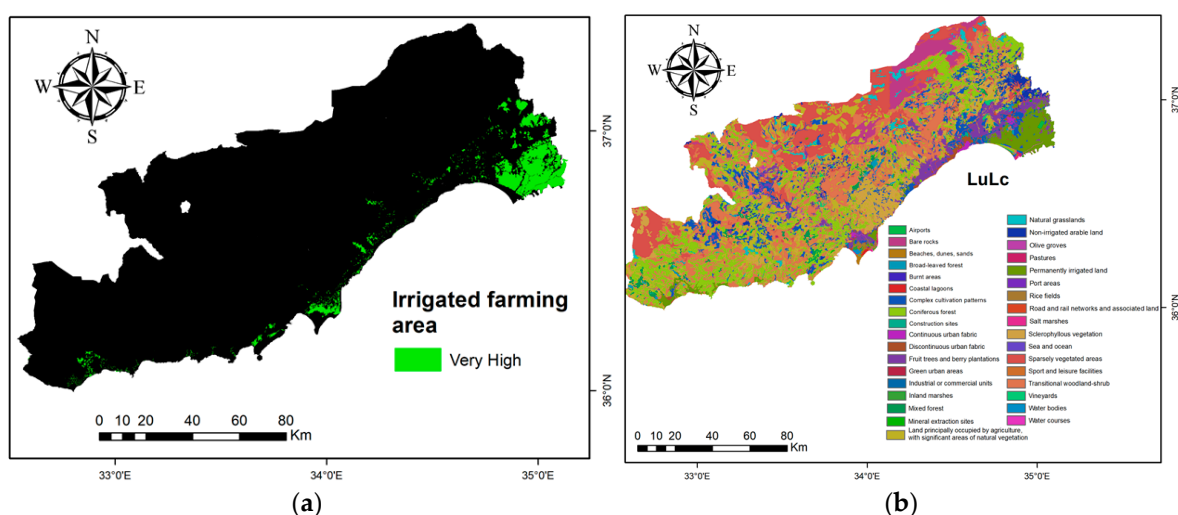


Figure 6. (a) Irrigated farming areas and (b) LuLc.

##### Land Use/Land Cover (LuLc)

LuLc is a parameter that affects the percolation of water into the ground, according to human activity [71]. The LuLc includes water flow, the percolation of water, and

permeability [72]. The LuLc layer was obtained from the CLMS (Figure 6b). The layer contains 35 classes.

### 3.2. AHP

The AHP is a method that uses a multicriteria decision if experts’ opinions are necessary, and the method utilizes a pairwise comparison matrix and determining weights [73]. The AHP approach is utilized in a variety of applications, including optimal location analysis; flood, landslide, and sinkhole risk assessments; demography analysis; and resource estimation (natural or artificial). It also enables numerous analyses to be conducted in different professional disciplines [15–17,73,74]. It is the appropriate method for solving multicriteria problems [74,75]. The weights are determined by the significance levels of the parameters in the AHP [76,77]. The significance levels and the weights of the parameters were determined in the study using experts and the literature. Interviews were conducted with three experts: two from the Republic of Türkiye General Directorate of State Hydraulic Works (RTGDSHW) and one from the Mersin Water and Sewerage Administration General Directorate (MWSGD). Thus, Table 6 was produced using the data from these interviews and studies from the literature.

Some basic steps must be followed to implement the AHP. The first step is to define the problem and construct a hierarchical structure. The most significant component in decision making is the hierarchical structure, and identifying incorrect or missing structures is indeed the biggest obstacle to decision making.

A pairwise comparison matrix is created after determining the parameters. In a problem with n parameters, n(n–1)/2 comparisons are made, and a pairwise comparison matrix of size n x n is generated. The 1–9 significance scale suggested by Saaty (1987) is used to compare the parameters [78]. It is shown in Table 3.

**Table 3.** Values on the Saaty scale.

Less Important				Equal Important	Intermediate Values				More Important			
EI	VHI	VI	MI		MI	VI	VHI	EI				
1/9	1/7	1/5	1/3	1	2	4	6	8	3	5	7	9

EI: extremely important; VHI: very highly important; VI: very important; and MI: moderately important.

The normalized weights are found after the pairwise comparison matrix has been constructed. They are determined by taking the geometric mean of these parameters (Equation (7)).

$$W_n = \frac{G_m}{\sum_{i=1}^n G_m} \tag{7}$$

where W is the weight vector, and G<sub>m</sub> is the geometric mean.

A consistency analysis is carried out using the weighted pairwise comparison matrix to ensure the accuracy of the AHP results. The analysis employs the consistency index (CI) (Equation (8)) and the consistency ratio (CR) (Equation (9)). The comparison matrix is allowed if the CR is 0.10 or less; otherwise, the comparison matrix will need to be updated. In the study, the CR was calculated to be 0.06 (Table 4).

$$\lambda_{max} = 1/n \sum_{i=1}^n (A_w)_i / w_i \tag{8}$$

$$CI = (\lambda_{max} - n) / (n - 1) \tag{9}$$

$$CR = CI / RI \tag{10}$$

In Equations (9) and (10), λ<sub>max</sub> is the maximum eigenvalue of the matrix, and n is the size of the matrix. In Equation (4), RI is a random index; the RI values are presented in Table 5.

**Table 4.** Pairwise comparison decision matrix ( $\lambda_{max}$ ), consistency index (CI), random consistency index (RI), and consistency ratio (CR).

GWPZ	$\lambda_{max}$	CI	RI	CR
	16.252	0.089	1.59	0.056

**Table 5.** Random index values.

n	1	2	3	4	5	6	7	8	9	10	11	12	13	14	15
RI	0	0	0.58	0.9	1.12	1.24	1.32	1.41	1.45	1.51	1.52	1.54	1.56	1.58	1.59

The ultimate step after determining the parameters is to generate a GWPZ map with a combination of parameters (Table 6). The WOT was utilized in this phase. The goal was to create a GWPZ suitability index by taking the sum of the parameters (Table 7). The index is calculated by multiplying the parameter weight values by the parameter sub-scores (Equation (11)).

$$GWPZ_i = \sum_{i=1}^n w_i r_i \tag{11}$$

where  $n$  represents the number of parameters,  $w_i$  is the weight of the  $i$ th parameter, and  $r_i$  is the parameter rating.

**Table 6.** Pairwise comparison matrices and main weights for the identification of groundwater potential zones.

Parameters	A	B	C	D	E	F	G	H	I	J	K	L	M	N	O	$W_i$
Water Resources (A)	1															0.177
Rainfall (B)	1	1														0.175
Irrigated Farming Areas (C)	1/2	1/2	1													0.094
Plains (D)	1/4	1/4	1/3	1												0.065
Drainage Density (E)	1/5	1/5	1/4	1/2	1											0.054
Lineament Density (F)	1/5	1/5	1/4	1/2	1	1										0.052
Geology (G)	1/3	1/3	2	3	2	2	1									0.088
Slope (H)	1/4	1/4	1/2	1/2	1/2	1/2	1/2	1								0.043
Soil (I)	1/3	1/3	2	3	3	3	1	2	1							0.091
TWI (J)	1/5	1/5	1/4	1/3	1/3	1/3	1/3	1/2	1/3	1						0.023
SPI (K)	1/5	1/5	1/3	1/3	1/3	1/3	1/3	1/2	1/3	1	1					0.024
STI (L)	1/5	1/5	1/3	1/3	1/3	1/2	1/3	1/2	1/2	1	1	1				0.026
LuLc (M)	1/7	1/6	1/3	1/4	1/2	1/2	1/2	1/2	1/2	2	2	2	1			0.036
Water Erosion (N)	1/5	1/5	1/3	1/3	1/3	1/3	1/4	1/2	1/4	2	2	1	1/2	1		0.029
TRI (O)	1/5	1/5	1/3	1/3	1/3	1/3	1/3	1/2	1/3	1	1	1	1/2	1/2	1	0.024

**Table 7.** Weightings and values of the parameters.

Parameters	Sub-Classes	Value
Water Resources	Stream	5
	River	5
	Water bodies	5
	Canal	4
	Dam	4
	Lake	5
	Pond	3

Table 7. Cont.

Parameters	Sub-Classes	Value
Rainfall	Very high	5
	High	4
	Moderate	3
	Low	2
	Very low	1
Irrigated Farming Areas	Very high	5
Plains	Very high	5
Drainage Density	Very high	1
	High	2
	Moderate	3
	Low	4
	Very low	5
Lineament Density	Very high	5
	High	4
	Moderate	3
	Low	2
	Very low	1
Geology	Cenozoic–Mesozoic intrusive rocks	1
	Devonian	2
	Jurassic	3
	Cretaceous	2
	Cretaceous–Jurassic	2
	Mesozoic	1
	Mesozoic–Paleozoic	1
	Neogene	2
	Permian	2
	Paleogene	2
	Precambrian–Paleozoic	4
	Upper Paleozoic	3
	Undivided Quaternary	4
	Sea and large lakes	5
	Triassic	2
Unmapped Area	1	
Slope	0–1	5
	1–2	4
	2–3	3
	3–4	2
	4–5	2
	>5	1
Soil	Alluvial soil	5
	Beach sand, dunes, and marsh soil	4
	Halomorphic soil	3
	Hydromorphic saline soil	5
	Red podzolic soil	1
	Terra rose soil	2
	Moderately sloping terra rose soil	2
	Volcanic and igneous rock soil	1
TWI	Very high	5
	High	4
	Moderate	3
	Low	2
	Very low	1

Table 7. Cont.

Parameters	Sub-Classes	Value
SPI	Very high	5
	High	4
	Moderate	3
	Low	2
	Very low	1
STI	Very high	5
	High	4
	Moderate	3
	Low	2
	Very low	1
Water Erosion	Very high	2
	High	3
	Moderate	4
	Never or very low	5
TRI	Very high	5
	High	4
	Moderate	3
	Low	2
	Very low	1
LuLc	Airports	1
	Bare rocks	1
	Beaches, dunes, sands	4
	Broad-leaved forest	3
	Burnt areas	1
	Coastal lagoons	5
	Complex cultivation patterns	2
	Coniferous forest	3
	Continuous urban fabric	1
	Fruit trees and berry plantations	3
	Green urban areas	1
	Inland marshes	5
	Land principally occupied by agriculture, with significant areas of natural vegetation	5
LuLc	Mineral extraction sites	1
	Mixed forest	2
	Natural grasslands	3
	Non-irrigated arable land	1
	Pastures	4
	Permanently irrigated land	5
	Port areas	5
	Rice fields	5
	Road and rail networks and associated land	1
	Salt marshes	2
	Sclerophyllous vegetation	3
	Sea and ocean	4
	Sparsely vegetated areas	2
	Transitional woodland-shrub	3
	Vineyards	2
	Water bodies	5
	Water courses	5

The AHP technique was primarily used to calculate the GWPZs, which is the study's ultimate goal. Weights were assigned to these fifteen layers using the AHP method. The weighted overlay technique (WOT) was used for the layers once the weights were assigned [7,13,79,80]. Thus, the GWPZs were computed using Equation (11).

### 3.3. VIKOR

The VIKOR method is a multi-criteria decision-making (MCDM) method developed by Duckstein and Opricovic in 1980. The VIKOR approach is used to identify alternative solutions. The relative distance between the ideal best and worst solutions is calculated, and the parameters are weighted accordingly [81]. This method, which can be applied in a variety of settings and allows for successful analyses and predictions, is also gaining popularity due to its consistent findings in determining groundwater zones [23]. Due to these characteristics, it was chosen as one of the approaches to GWPZ detection for the study.

To calculate the VIKOR, the first step is to generate a decision matrix (Equation (12)). In the following processing step, a normalized decision matrix is created (Table 8). The best and worst ideal solutions are calculated (Equations (13) and (14)). Values are calculated to rank all the solutions (Equations (15) and (16)). The final calculation is executed during the last processing step. (Equation (17)). Thus, the solutions are sorted, and their values are obtained (Tables 9 and 10).

$$f_{ij} = x_{ij} / \sqrt{\sum_{j=1}^m x_{ij}^2} \quad (i = 1, 2, \dots, m; j = 1, 2, \dots, n) \quad (12)$$

where  $f_{ij}$  represents the normalized value of  $x$ .

$$f_i^+ = \begin{Bmatrix} \max f_{ij} \\ i \\ \min f_{ij} \\ i \end{Bmatrix} \quad (13)$$

$$f_i^- = \begin{Bmatrix} \min f_{ij} \\ i \\ \max f_{ij} \\ i \end{Bmatrix} \quad (14)$$

where  $f_i^+$  is the distance between the best ideal solutions, and  $f_i^-$  is the distance between the worst ideal solutions.

$$S_j = \sum_{i=1}^n \left[ \frac{w_i (f_i^* - f_{ij})}{(f_i^* - f_i^-)} \right] \quad (15)$$

$$R_j = \max_i \left[ \frac{w_i (f_i^* - f_{ij})}{(f_i^* - f_i^-)} \right] \quad (16)$$

where  $w_i$  represents the weight of the  $i$ th parameter, and  $S_j$  and  $R_j$  represent the ranks of the parameters.

$$\begin{aligned} Q_j &= v \left[ \frac{(S_j - S^+)}{(S^- - S^+)} \right] + (1 - v) \left[ \frac{(R_j - R^+)}{(R^- - R^+)} \right] \\ S^+ &= \min \left[ (S_j) \mid j = 1, 2, \dots, m \right] \\ S^- &= \max \left[ (S_j) \mid j = 1, 2, \dots, m \right] \\ R^+ &= \min \left[ (R_j) \mid j = 1, 2, \dots, m \right] \\ R^- &= \max \left[ (R_j) \mid j = 1, 2, \dots, m \right] \end{aligned} \quad (17)$$

where  $v$  is the subjectively defined weight, which can range between 0 and 1. In the study, 0.5 was used for each parameter.

**Table 8.** Normalized decision matrix.

	A	B	C	D	E	F	G	H	I	J	K	L	M	N	O
A	0.795	0.795	0.795	0.619	0.619	0.530	0.442	0.354	0.265	0.265	0.265	0.177	0.177	0.088	0.088
B	0.398	0.398	0.354	0.309	0.309	0.265	0.221	0.177	0.133	0.133	0.133	0.088	0.088	0.044	0.044
C	0.265	0.265	0.236	0.206	0.206	0.177	0.147	0.118	0.088	0.088	0.088	0.059	0.059	0.029	0.029
D	0.199	0.199	0.177	0.155	0.155	0.133	0.110	0.088	0.066	0.066	0.066	0.044	0.044	0.022	0.022
E	0.159	0.159	0.141	0.124	0.124	0.106	0.088	0.071	0.053	0.053	0.053	0.035	0.035	0.018	0.018
F	0.133	0.133	0.118	0.103	0.103	0.088	0.074	0.059	0.044	0.044	0.044	0.029	0.029	0.015	0.015
G	0.114	0.114	0.101	0.088	0.088	0.076	0.063	0.051	0.038	0.038	0.038	0.025	0.025	0.013	0.013
H	0.099	0.099	0.088	0.077	0.077	0.066	0.055	0.044	0.033	0.033	0.033	0.022	0.022	0.011	0.011
I	0.088	0.088	0.079	0.069	0.069	0.059	0.049	0.039	0.029	0.029	0.029	0.020	0.020	0.010	0.010
J	0.080	0.080	0.071	0.062	0.062	0.053	0.044	0.035	0.027	0.027	0.027	0.018	0.018	0.009	0.009
K	0.072	0.072	0.064	0.056	0.056	0.048	0.040	0.032	0.024	0.024	0.024	0.016	0.016	0.008	0.008
L	0.066	0.066	0.059	0.052	0.052	0.044	0.037	0.029	0.022	0.022	0.022	0.015	0.015	0.007	0.007
M	0.061	0.061	0.054	0.048	0.048	0.041	0.034	0.027	0.020	0.020	0.020	0.014	0.014	0.007	0.007
N	0.057	0.057	0.051	0.044	0.044	0.038	0.032	0.025	0.019	0.019	0.019	0.013	0.013	0.006	0.006
O	0.053	0.053	0.047	0.041	0.041	0.035	0.029	0.024	0.018	0.018	0.018	0.012	0.012	0.006	0.006

**Table 9.** Alternative solutions.

	A	B	C	D	E	F	G	H	I	J	K	L	M	N	O
$S_j$	3.755	1.877	1.269	1.001	0.751	0.626	0.501	0.501	0.375	0.375	0.375	0.375	0.250	0.250	0.250
$R_j$	0.300	0.150	0.100	0.080	0.060	0.050	0.040	0.040	0.030	0.030	0.030	0.030	0.020	0.020	0.020

**Table 10.**  $Q_j$  values ( $v = 0.5$ ).

A	B	C	D	E	F	G	H	I	J	K	L	M	N	O
1	0.464	0.288	0.214	0.143	0.107	0.071	0.071	0.036	0.036	0.036	0.036	0	0	0

### 3.4. TOPSIS

Hwang and Yoon developed the TOPSIS, an MCDM approach, in 1981 [82]. This technique provides several solution alternatives by ordering criteria based on Euclidean distances. The order of the criteria created according to distance is the minimum distance to the positive ideal solution and the maximum distance to the negative ideal solution [83,84]. Thus, comparing positive and negative ideal solutions yields optimal results [85]. The TOPSIS approach produces successful results in a wide range of fields, including agricultural practices, economic studies, capacity estimation of energy resources, and groundwater research [21,86,87]. In this study, it was selected as one of the options for GWPZ detection.

The decision matrix for the TOPSIS calculation is initially generated using Equation (18), as in the VIKOR approach (Table 8). Weights are assigned to the decision matrix (Equation (19)), positive and negative ideal solutions are determined (Equations (20) and (21)), the distances between the positive and negative ideal solutions are calculated (Equations (22) and (23)), and finally, the method’s performance score is computed (Equation (24)). Thus, the highest value of the performance score indicates a high GWPZ, while the lowest number suggests a low GWPZ.

$$V_{ij} = P_{ij} / \sqrt{\sum_{i=1}^m P_{ij}^2} (i = 1, 2, \dots, m; j = 1, 2, \dots, n) \tag{18}$$

where  $V_{ij}$  represents the normalized value of  $P_{ij}$ .

$$V_{m \times n} = N_{m \times n} W_{n \times n} \tag{19}$$

where  $V_{m \times n}$  refers to the weighted normalized matrix (Table 11), and  $W_{n \times n}$  refers to the weight matrix.

$$V^+ = \{v_1^+, v_2^+, \dots, v_n^+\} = \left\{ (max v_{ij} \mid j \in I), (min v_{ij} \mid j \in I^1) \right\} \tag{20}$$

$$V^- = \{v_1^-, v_2^-, \dots, v_n^-\} = \left\{ (min v_{ij} \mid j \in I), (max v_{ij} \mid j \in I^1) \right\} \tag{21}$$

where  $V^+$  is the positive ideal solution,  $V^-$  is the negative ideal solution,  $I$  is the utility feature, and  $I^1$  is the cost feature.

$$d_i^+ = \sqrt{\sum_{j=1}^n (v_{ij} - v_j^+)^2} \quad (i = 1, \dots, m; j = 1, \dots, n) \tag{22}$$

$$d_i^- = \sqrt{\sum_{j=1}^n (v_{ij} - v_j^-)^2} \quad (i = 1, \dots, m; j = 1, \dots, n) \tag{23}$$

where  $d_i^+$  represents the distance between positive ideal solutions, and  $d_i^-$  represents the distance between negative ideal solutions.

$$p_i = \frac{d_i^-}{(d_i^+ + d_i^-)} \quad (i = 1, \dots, m) \tag{24}$$

where the performance score is shown as  $p_i$  (Table 12).

**Table 11.** Weighted normalized decision matrix.

	A	B	C	D	E	F	G	H	I	J	K	L	M	N	O
A	0.239	0.119	0.080	0.049	0.037	0.027	0.018	0.014	0.008	0.008	0.008	0.005	0.004	0.002	0.002
B	0.119	0.060	0.035	0.025	0.019	0.013	0.009	0.007	0.004	0.004	0.004	0.003	0.002	0.001	0.001
C	0.080	0.040	0.024	0.016	0.012	0.009	0.006	0.005	0.003	0.003	0.003	0.002	0.001	0.001	0.001
D	0.060	0.030	0.018	0.012	0.009	0.007	0.004	0.004	0.002	0.002	0.002	0.001	0.001	0.000	0.000
E	0.048	0.024	0.014	0.010	0.007	0.005	0.004	0.003	0.002	0.002	0.002	0.001	0.001	0.000	0.000
F	0.040	0.020	0.012	0.008	0.006	0.004	0.003	0.002	0.001	0.001	0.001	0.001	0.001	0.000	0.000
G	0.034	0.017	0.010	0.007	0.005	0.004	0.003	0.002	0.001	0.001	0.001	0.001	0.001	0.000	0.000
H	0.030	0.015	0.009	0.006	0.005	0.003	0.002	0.002	0.001	0.001	0.001	0.001	0.000	0.000	0.000
I	0.027	0.013	0.008	0.005	0.004	0.003	0.002	0.002	0.001	0.001	0.001	0.001	0.000	0.000	0.000
J	0.024	0.012	0.007	0.005	0.004	0.003	0.002	0.001	0.001	0.001	0.001	0.001	0.000	0.000	0.000
K	0.022	0.011	0.006	0.004	0.003	0.002	0.002	0.001	0.001	0.001	0.001	0.000	0.000	0.000	0.000
L	0.020	0.010	0.006	0.004	0.003	0.002	0.001	0.001	0.001	0.001	0.001	0.000	0.000	0.000	0.000
M	0.018	0.009	0.005	0.004	0.003	0.002	0.001	0.001	0.001	0.001	0.001	0.000	0.000	0.000	0.000
N	0.017	0.009	0.005	0.004	0.003	0.002	0.001	0.001	0.001	0.001	0.001	0.000	0.000	0.000	0.000
O	0.016	0.008	0.005	0.003	0.002	0.002	0.001	0.001	0.001	0.001	0.001	0.000	0.000	0.000	0.000

**Table 12.** Solutions ( $V^+$ ,  $V^-$ ), distances between solutions ( $d_i^+$ ,  $d_i^-$ ), and performance score ( $p_i$ ) values.

	A	B	C	D	E	F	G	H	I	J	K	L	M	N	O
$V^+$	0.239	0.119	0.080	0.049	0.037	0.027	0.018	0.014	0.008	0.008	0.008	0.005	0.004	0.002	0.002
$V^-$	0.016	0.008	0.005	0.003	0.002	0.002	0.001	0.001	0.001	0.001	0.001	0.000	0.000	0.000	0.000
$d_i^+$	1.064	0.532	0.362	0.221	0.166	0.118	0.079	0.063	0.035	0.035	0.035	0.024	0.016	0.008	0.008
$d_i^-$	0.262	0.131	0.085	0.054	0.041	0.029	0.019	0.016	0.009	0.009	0.009	0.006	0.004	0.002	0.002
$p_i$	0.197	0.197	0.200	0.185	0.190	0.200	0.200	0.250	0.200	0.200	0.200	0.333	0.000	0.000	0.197

### 3.5. Validation

Validation is a critical component for modeling the reliability and consistency of scientific research [88,89]. Given the process that serves as the study's major axis and the methods utilized to carry it out, the receiver operating characteristic (ROC) curve is mostly selected for validation [23,90–92]. The area under the curve (AUC) value measures prediction accuracy [93,94]. The ROC curve's y-axis indicates the true positive rate, while the x-axis represents the true negative rate. The AUC value varies from 0 to 1. Values near one suggest that the model performs better and is more reliable. In this study, the ROC curve was utilized to validate the GWPZ models produced using the various approaches.

## 4. Results

The GWPZ maps were created utilizing fifteen thematic layers (Figure 7). Each GWPZ map was organized into five classes ("Very High", "High", "Moderate", "Low", and "Very Low").

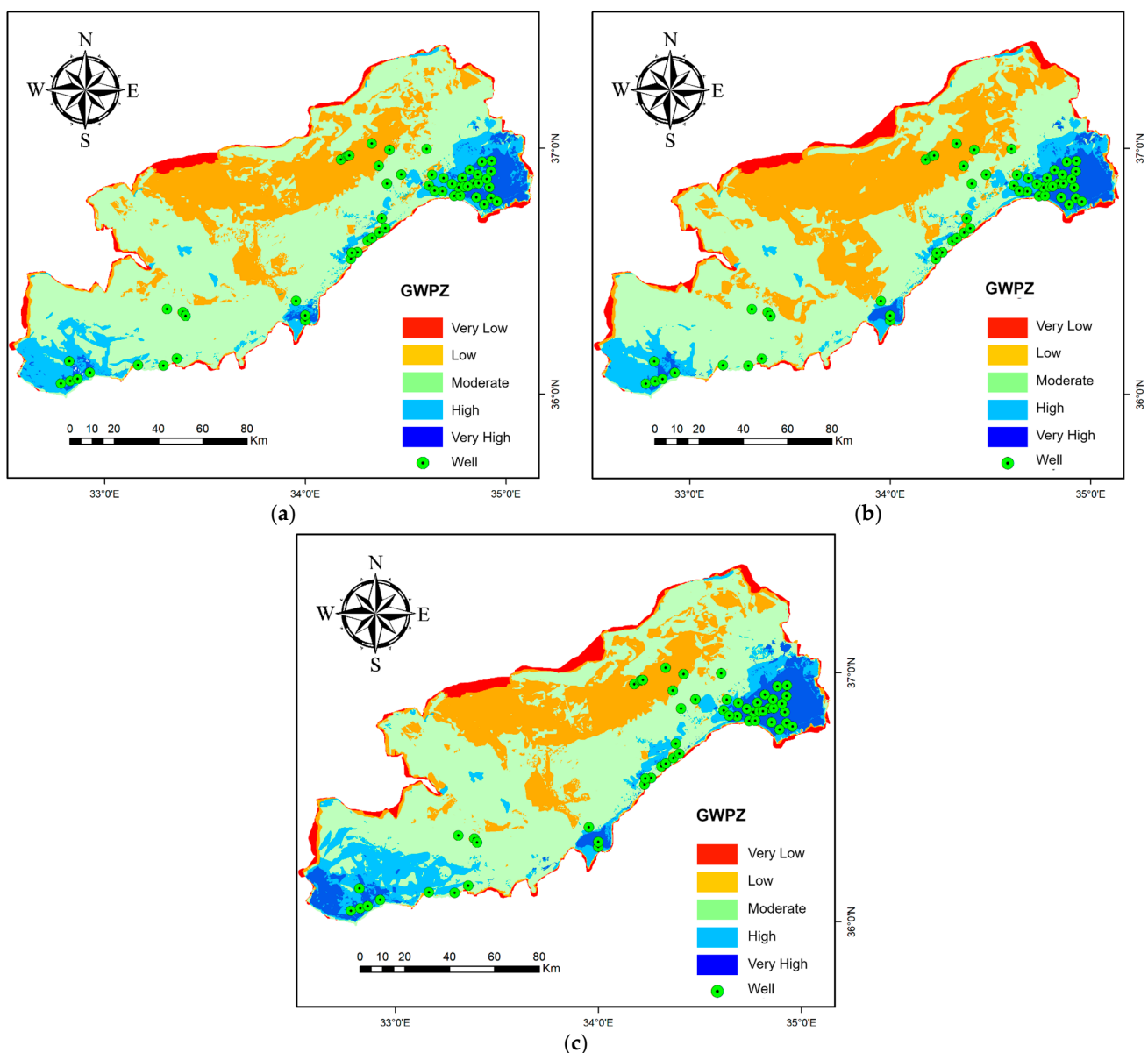


**Figure 7.** (a) Groundwater potential maps of the study area obtained by the (a) AHP, (b) VIKOR, and (c) TOPSIS methods.

A “Very High” GWPZ is categorized as having a gentle slope, a low drainage density, high levels of water erosion, a high lineament density, high levels of rainfall, and a high TWI, TRI, SPI, and STI. “Very High” GWPZs make up 4.98%, 5.94%, and 7.96% of the study area in turn (according to the AHP, VIKOR, and TOPSIS methods). The middle of the study area has 450–700 mm of annual average rainfall and a moderate lineament density; hence, it is classified as a “Moderate” GWPZ (60.68%, 52.41%, 51.56%). The “Low” and “Very Low” GWPZ classes have inverse features to the “Very High” class, and they have less recharge capacity [31]. The north of the study area and hilly places have steep slopes. They have unsuitable geological formations and soil textures, so they are classified as “Low” (21.28%, 28.53, 20.90%) and “Very Low” (2.18%, 2.80%, 3.07%) GWPZs (Table 13).

**Table 13.** Classifications of groundwater potential zones.

Classes	AHP		VIKOR		TOPSIS	
	Area (km <sup>2</sup> )	% Area	Area (km <sup>2</sup> )	% Area	Area (km <sup>2</sup> )	% Area
Very Low	345.23	2.18	443.38	2.80	487.38	3.07
Low	3373.18	21.28	4522.26	28.53	3313.61	20.90
Moderate	9618.81	60.68	8309.08	52.41	8173.84	51.56
High	1727.05	10.89	1636.26	10.32	2616.04	16.50
Very High	788.73	4.98	942.01	5.94	1262.14	7.96
<b>Total</b>					15,853	100

Data from 60 wells in the study area were utilized to validate the GWPZ analysis. The wells in the study area were received from RTGDSHW together with location data. Wells are recognized as indicators of the probable existence of groundwater [7,13,94]. Therefore, they were used to verify the GWPZs. Two steps were determined for this aim. Firstly, GWPZ classes and well locations were established (Figure 8).

The GWPZ maps generated were then confirmed with the ROC curve. The test data consisted of 60 wells. AUC values were determined for the AHP, VIKOR, and TOPSIS techniques, respectively (Figure 9). When the resulting values were analyzed, it was discovered that all three procedures produced similar results. The VIKOR methodology was determined to be the most accurate (76.5%). Although the TOPSIS approach had fairly similar values to the other two methods, it was found to have the lowest AUC value among these GIS-based methods (76.1%).

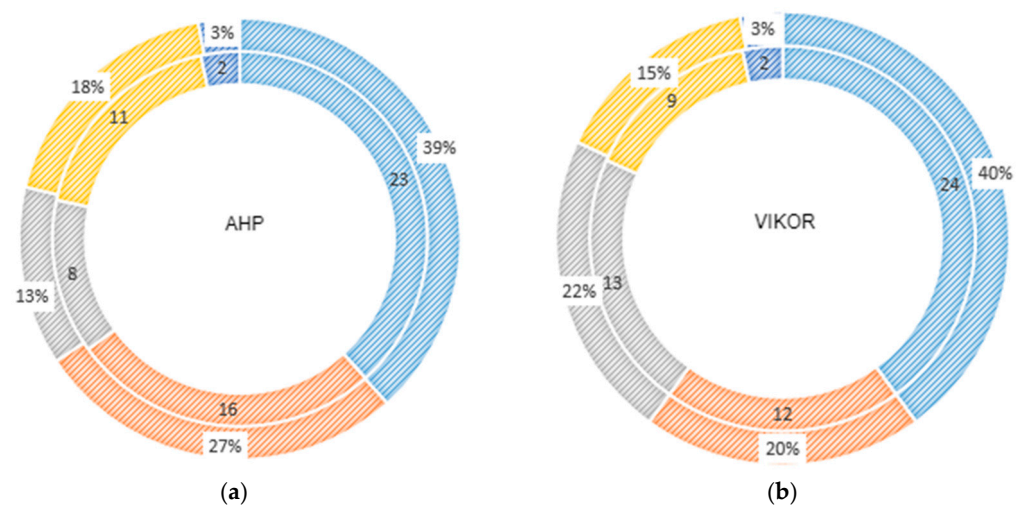


**Figure 8.** Cont.

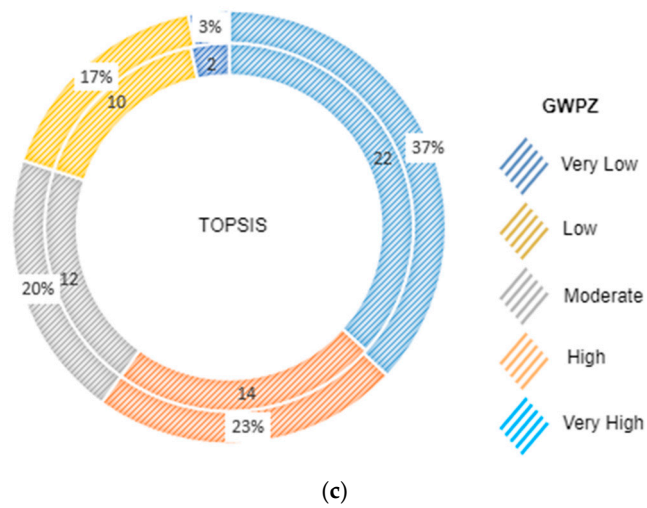


Figure 8. The numbers and percentages of wells in GWPZ classes obtained as a result of (a) the AHP, (b) VIKOR, and (c) TOPSIS methods.

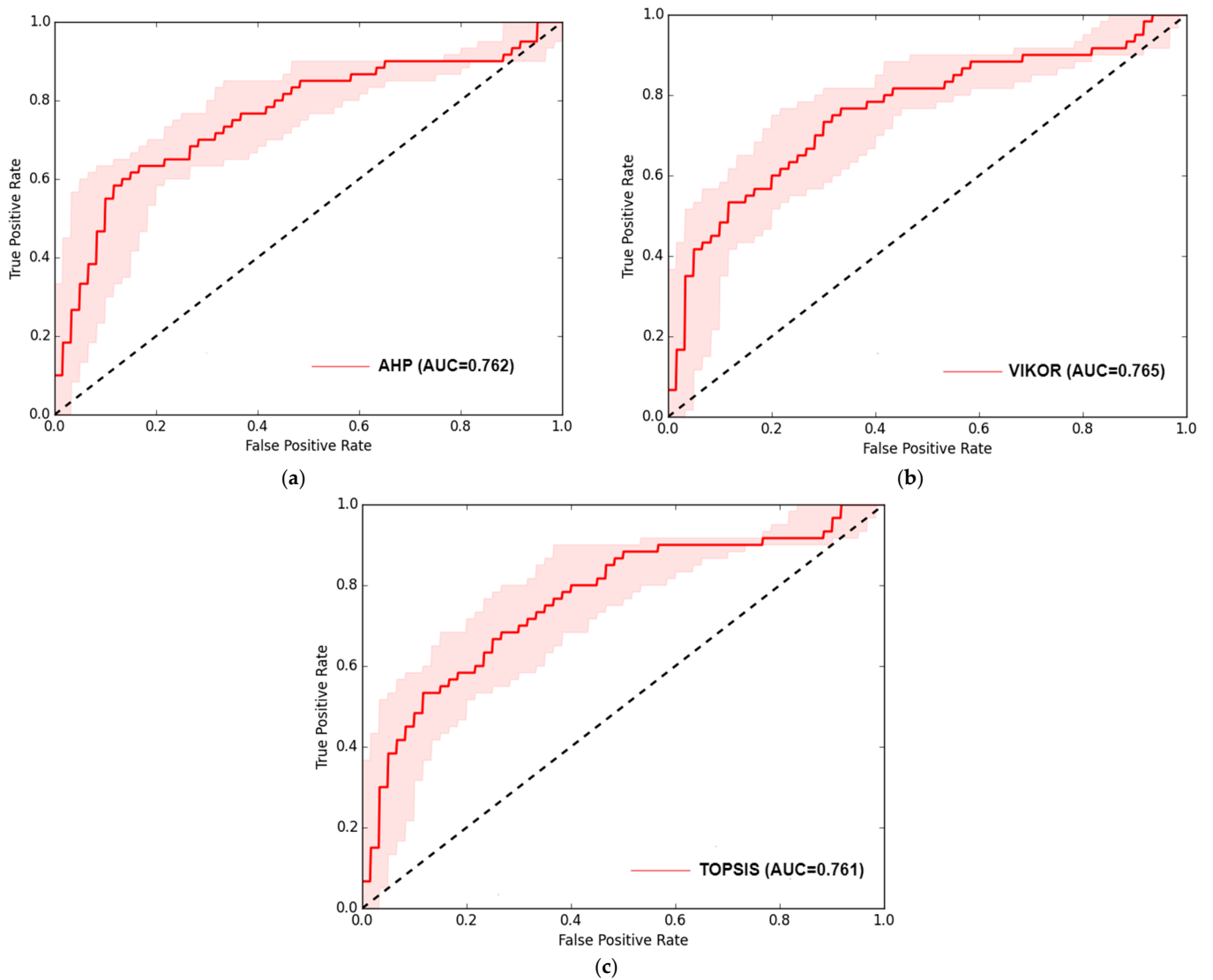


Figure 9. Validation of the (a) AHP, (b) VIKOR, and (c) TOPSIS methods with ROC curve.

## 5. Discussion

According to [28], in a study conducted in the Barind tract in the northwestern part of Bangladesh, 4% of the study area was classified as “very high” and 13% as “high” GWPZs, and [95] discovered that 19.34% of a study area in Dak Nong Province, Vietnam, has a “high” groundwater potential. According to [66], in a study performed in Ethiopia’s Beles River Basin, it was stated that approximately 19% of the region has “good” groundwater potential. Furthermore, [32] found that around 6% to 18% of the area is classified as “very high” or “high” GWPZs. In our study, 4.98%, 5.94, and 7.96% of the study area were classified as “Very High,” with 10.89%, 10.32%, and 16.50% classified as “High”, respectively.

It was seen that GWPZ research has extensively used 5–8 parameters when previous studies were investigated [30,32,96–98]. On the other hand, several studies have utilized more parameters for GWPZ detection [99,100]. It was determined that LuLc, soil, drainage density, lineament density, and geology are standard parameters and essential when GWPZ studies are examined. Refs. [31,36] considered rainfall and drainage density relevant. The annual average rainfall is 613.2 mm in Mersin; therefore, rainfall was an excellent parameter for GWPZ detection in our study. However, more is needed to determine groundwater potential [55] because a region that has much rainfall does not always point to the presence of groundwater [101]. The soil diversity and texture in a region (TRI) [102], land use, geological texture, abrasive power of water (SPI) [67], water-holding capacity (STI) [66], quantity of percolation (DD) [31], and inflow (TWI) [55] directly affect the groundwater potential. For these reasons, the stated rainfall parameter and other parameters should be considered jointly for an optimum GWPZ analysis. The mentioned parameters were also used in the study, and the GWPZs were tested to determine them precisely.

Their resolution is as important as the number of parameters utilized. It is a vital component in ensuring the consistency of the analysis. Ref. [30] employed parameters that can be considered high-resolution (30 m) for GWPZ detection in the Darjeeling Himalayan region of India. Likewise, in a study conducted in [32] in southern Aseer, southwestern Saudi Arabia, and in a study conducted in [96] in the Gandheswari watershed, West Bengal, 30 m-resolution satellite images were used. In this study, high-resolution parameters were similarly chosen for the accuracy of GWPZ detection in the study area.

Fifteen parameters that are GIS-based were used in the study, and GWPZ maps were created. Unlike previous investigations, fifteen parameters were evaluated for precision and high accuracy. Not only did the number of parameters employed differ from other studies, so did the validation analysis. Although they employed parameters ranging from 10 to 12, [100] did not perform any validation. On the other hand, [36,57,96,97,103] used few parameters (5–8) despite their validation. A significant number of parameters were used in this study, and validation was carried out.

In this study, the GIS-based AHP, VIKOR, and TOPSIS techniques were utilized to detect GWPZs in the study area. In this regard, the study presents analyses that can be compared to one another and distinguished from many other studies. The studies carried out in [30,32,34,96,104] used just the AHP approach. There are also numerous studies that use only the VIKOR [19,105–107] and TOPSIS [21,84,86,87] methods. There have been few studies combining multiple approaches. Ref. [23] employed TOPSIS and VIKOR algorithms in their research. The models were validated using the ROC curve. The values were 86.7% and 70.2%, respectively. In that regard, this study differs from our research. Ref. [81] chose to use the TOPSIS and VIKOR approaches.

This study involved an application on a Mersin provincial scale. Studies have been carried out on part of the study area previously. However, no studies of this magnitude have been conducted throughout Mersin. Ref. [108] researched groundwater and pollution in the Göksu Delta, Silifke district. The study in [109] focused on a coastal aquifer in Tarsus district. Ref. [110]’s study is noteworthy as it was also performed in Mersin. The study assessed the potential groundwater in the Akdere and Yeşilovacık neighborhoods in Silifke district using the AHP method and nine factors. In this study, GWPZ determination was carried out inside the confines of Mersin province with the AHP, VIKOR, and TOPSIS methods.

Moreover, Mersin confronts water requirement (drinking, agriculture, and industry) problems owing to its increasing population, industrialization, drought, and global climate change [111]. These situations are increasing the use of groundwater. As [49] stated, determining and monitoring groundwater levels is vital for the sustainable use of groundwater. Uncontrolled and frequent groundwater use can cause adverse incidents, particularly in drylands like Mersin, which has a drought risk [112]. Water resources should be utilized optimistically as part of sustainable groundwater management [113,114].

Groundwater management should be conducted with scientific norms and innovative methods for sustainable groundwater resources [6]. Groundwater's long-term use and strategic importance are precious for decision makers and policymakers regarding sustainable groundwater management [36]. As [31] stated, sustainable groundwater management should be carried out according to each groundwater feature. Factors like the usage of groundwater, quality, pollution, connected streams, and the ecosystem should be considered [115–117]. The scientific procedures used in groundwater extraction are substantial for groundwater management, and the development of management plans will have a good impact on the groundwater protection–use balance and improvement.

The groundwater potential zones were identified using several criteria in this study, and validation was performed. Attention was drawn to sustainable groundwater management, as managing these areas was as crucial as identifying potential groundwater zones.

## 6. Conclusions

Groundwater usage, protection, and management effectively satisfy water requirements and prevent future generations from suffering in the context of sustainable groundwater management. In this regard, optimizing groundwater use, avoiding waste, and reducing the water footprint in the study area where agricultural activities are carried out effectively are critical. The first stage in this framework is the determination of groundwater and groundwater recharge zones. The processes for determining management, use, and protection policies follow. A GIS allows for spatial and visual inferences. In addition, it is a dependable and cost-effective tool. Various analyses can be performed by integrating the AHP, VIKOR, and TOPSIS into this tool. In this study, these methods were used. The GWPZs in Mersin were determined, which face drought and global climate change threats. The attained results were divided into five classes. The GWPZ models were then validated with well data in the study area. Nonetheless, in studies where the wells in the GWPZs are specifically assessed, GWPZ determination should be conducted using data such as the well discharge, the yield of the well, and the depth level of the groundwater. In this manner, the validation will be more accurate. The analysis will improve when more wells are used. In the absence of such data, the proposed methodology and the parameters are among the leading methods for assessing groundwater potential.

The study contributes fundamental knowledge to engineers, hydrologists, and water management decision makers. This will allow people to make rapid and accurate decisions. Furthermore, it will help to ensure that applications are implemented properly. In this regard, it is considered to play a vital role in balancing time and cost. We think that the parameters used in the study are appropriate to utilize without any alteration in regions with drought and climate change.

**Author Contributions:** Conceptualization, M.Ö.Ç. and L.K.; data curation, M.Ö.Ç. and L.K.; methodology, M.Ö.Ç., L.K. and M.Y.; writing—original draft preparation, M.Ö.Ç. and L.K., writing—review and editing, M.Ö.Ç., L.K. and M.Y.; visualization, M.Ö.Ç. All authors have read and agreed to the published version of the manuscript.

**Funding:** This research received no external funding.

**Institutional Review Board Statement:** Not applicable.

**Informed Consent Statement:** Not applicable.

**Data Availability Statement:** The data utilized in the study are available upon request from the corresponding author.

**Conflicts of Interest:** The authors declare no conflicts of interest.

## References

- Adere, T.H.; Mertens, K.; Maertens, M.; Vranken, L. The impact of land certification and risk preferences on investment in soil and water conservation: Evidence from southern Ethiopia. *Land Use Policy* **2022**, *123*, 106406. [CrossRef]
- Han, D.; Currell, M.J. Persistent organic pollutants in China's surface water systems. *Sci. Total Environ.* **2017**, *580*, 602–625. [CrossRef]
- Kumar, V.; Parihar, R.D.; Sharma, A.; Bakshi, P.; Sidhu, G.P.S.; Bali, A.S.; Kargaouzas, I.; Bhardwaj, R.; Thukral, A.K.; Gyasi-Agyei, Y.; et al. Global evaluation of heavy metal content in surface water bodies: A meta-analysis using heavy metal pollution indices and multivariate statistical analyses. *Chemosphere* **2019**, *236*, 124364. [CrossRef]
- Dastgerdi, A.S.; Sargolini, M.; Allred, S.B.; Chatrchyan, A.M.; Drescher, M.; DeGeer, C. Climate change risk reduction in cultural landscapes: Insights from Cinque Terre and Waterloo. *Land Use Policy* **2022**, *123*, 106359. [CrossRef]
- Hutchinson, A.S.; Woodside, G.D.; Herndon, R.L. Increasing the Sustainable Yield of the Orange County Groundwater Basin with Managed Aquifer Recharge. *Groundwater* **2022**, *60*, 628–633. [CrossRef]
- Moraes-Santos, E.C.; Dias, R.A.; Balestieri, J.A.P. Groundwater and the water-food-energy nexus: The grants for water resources use and its importance and necessity of integrated management. *Land Use Policy* **2021**, *109*, 105585. [CrossRef]
- Roy, S.; Hazra, S.; Chanda, A.; Das, S. Assessment of groundwater potential zones using multi-criteria decision-making technique: A micro-level case study from red and lateritic zone (RLZ) of West Bengal, India. *Sustain. Water Resour. Manag.* **2020**, *6*, 4. [CrossRef]
- Tarback, E.J.; Lutgens, F.K.; Tasa, D.G. *Earth: An Introduction to Physical Geology*, 12th ed.; Pearson: London, UK, 2017.
- Taylor, R.G.; Scanlon, B.; Döll, P.; Rodell, M.; Van Beek, R.; Wada, Y.; Longuevergne, L.; Leblanc, M.; Famiglietti, J.S.; Edmunds, M.; et al. Ground water and climate change. *Nat. Clim. Chang.* **2013**, *3*, 322–329. [CrossRef]
- Li, P.; Qian, H.; Wu, J. Conjunctive use of groundwater and surface water to reduce soil salinization in the Yinchuan Plain, North-West China. *Int. J. Water Res. Dev.* **2018**, *34*, 337–353. [CrossRef]
- MAF. Ministry of agriculture and Forestry (MAF). Available online: <https://www.tarimorman.gov.tr/News/5217/325-Facilities-Put-Into-Service-On-The-World-Water-Day> (accessed on 20 January 2022).
- Agarwal, R.; Garg, P.K. Remote Sensing and GIS Based Groundwater Potential & Recharge Zones Mapping Using Multi-Criteria Decision Making Technique. *Water Resour Manag.* **2016**, *30*, 243–260. [CrossRef]
- Saranya, T.; Saravanan, S. Groundwater potential zone mapping using analytical hierarchy process (AHP) and GIS for Kancheepuram District, Tamilnadu, India. *Model. Earth Syst. Environ.* **2020**, *6*, 1105–1122. [CrossRef]
- Todd, D. *Groundwater Hydrology*; Wiley: New York, NY, USA, 1980; pp. 111–163.
- Bilgilioglu, S.S. Land suitability assessment for Olive cultivation using GIS and multi-criteria decision-making in Mersin City, Turkey. *Arab. J. Geosci.* **2021**, *14*, 2434. [CrossRef]
- Borah, H.; Deka, S. Exploration of Potential Zones of Groundwater in Jamuna Watershed, Assam, by Applying Multi-influencing Factor Technique. *J. Indian Soc. Remote Sens.* **2023**, *51*, 75–91. [CrossRef]
- Bozdog, A.; Ertunc, E. Real Property Valuation in the Sample of the City of Niğde through GIS and AHP Method. *J. Geomat.* **2020**, *5*, 228–240. [CrossRef]
- Dogan, Y.; Yakar, M. GIS and Three-Dimensional Modeling for Cultural Heritages. *Int. J. Eng. Geosci.* **2018**, *3*, 50–55. [CrossRef]
- Haider, H.; Ghumman, A.R.; Al-Salamah, I.S.; Thabit, H. Assessment framework for natural groundwater contamination in arid regions: Development of indices and wells ranking system using fuzzy VIKOR method. *Water* **2020**, *12*, 423. [CrossRef]
- Kusak, L.; Unel, F.B.; Alptekin, A.; Celik, M.O.; Yakar, M. Apriori association rule and K-means clustering algorithms for interpretation of pre-event landslide areas and landslide inventory mapping. *Open Geosci.* **2021**, *13*, 1226–1244. [CrossRef]
- Mandal, T.; Saha, S.; Das, J.; Sarkar, A. Groundwater depletion susceptibility zonation using TOPSIS model in Bhagirathi river basin, India. *Model. Earth Syst. Environ.* **2022**, *8*, 1711–1731. [CrossRef]
- Oguz, E.; Oguz, K.; Ozturk, K. Determination of flood susceptibility areas of Düzce region. *J. Geomat.* **2021**, *7*, 220–234. [CrossRef]
- Paul, S.; Roy, D. Geospatial modeling and analysis of groundwater stress-prone areas using GIS-based TOPSIS, VIKOR, and EDAS techniques in Murshidabad district, India. *Model. Earth Syst. Environ.* **2023**, *10*, 121–141. [CrossRef]
- Roy, K.C.; Barman, J.; Biswas, B. Multi-criteria decision-making for groundwater potentiality zonation in a groundwater scarce region in central India using methods of compensatory aggregating functions. *Groundw. Sustain. Dev.* **2024**, *25*, 101101. [CrossRef]
- Sari, F.; Sen, M. Least Cost Path Algorithm Design for Highway Route Selection. *Int. J. Eng. Geosci.* **2017**, *2*, 1–8. [CrossRef]
- Yıldırım, Ü. Evaluation of Groundwater Vulnerability in the Upper Kelkit Valley (Northeastern Turkey) Using DRASTIC and AHP-DRASTIC Models. *ISPRS Int. J. Geo-Inf.* **2023**, *12*, 251. [CrossRef]
- Yildirim, V.; Uzun, B.; Memisoglu Baykal, T.; Terzi, F.; Atasoy, B.A. Odor-aided analysis for landfill site selection: Study of DOKAP Region, Turkey. *Environ. Sci. Pollut. Res.* **2022**, *29*, 10754–10770. [CrossRef] [PubMed]
- Ferozur, R.M.; Jahan, C.S.; Arefin, R.; Mazumder, Q.H. Groundwater potentiality study in drought prone barind tract, NW Bangladesh using remote sensing and GIS. *Groundw. Sustain. Dev.* **2019**, *8*, 205–215. [CrossRef]

29. Yeh, H.F.; Cheng, Y.S.; Lin, H.I.; Lee, C.H. Mapping groundwater recharge potential zone using a GIS approach in Hualian River, Taiwan. *Sustain. Environ. Res.* **2016**, *26*, 33–43. [CrossRef]
30. Roy, S.; Bose, A.; Mandal, G. Modeling and mapping geospatial distribution of groundwater potential zones in Darjeeling Himalayan region of India using analytical hierarchy process and GIS technique. *Model. Earth Syst. Environ.* **2022**, *8*, 1563–1584. [CrossRef]
31. Patra, S.; Mishra, P.; Mahapatra, S.C. Delineation of groundwater potential zone for sustainable development: A case study from Ganga Alluvial Plain covering Hooghly district of India using remote sensing, geographic information system and analytic hierarchy process. *J. Clean. Prod.* **2018**, *172*, 2485–2502. [CrossRef]
32. Khan, M.Y.A.; ElKashouty, M.; Subyani, A.M.; Tian, F.; Gusti, W. GIS and RS intelligence in delineating the groundwater potential zones in Arid Regions: A case study of southern Aseer, southwestern Saudi Arabia. *Appl. Water Sci.* **2022**, *12*, 3. [CrossRef]
33. Al-Ruzouq, R.; Shanableh, A.; Yilmaz, A.G.; Idris, A.E.; Mukherjee, S.; Khalil, M.A.; Gibril, M.B.A. Dam site suitability mapping and analysis using an integrated GIS and machine learning approach. *Water* **2019**, *11*, 1880. [CrossRef]
34. Arulbalaji, P.; Padmalal, D.; Sreelash, K. GIS and AHP Techniques Based Delineation of Groundwater Potential Zones: A case study from Southern Western Ghats, India. *Sci. Rep.* **2019**, *9*, 2082. [CrossRef] [PubMed]
35. Mahmoud, S.H.; Alazba, A.A.; Amin, M.T. Identification of Potential Sites for Groundwater Recharge Using a GIS-Based Decision Support System in Jazan Region-Saudi Arabia. *Water Resour. Manag.* **2014**, *28*, 3319–3340. [CrossRef]
36. Ifediegwu, S.I. Assessment of groundwater potential zones using GIS and AHP techniques: A case study of the Lafia district, Nasarawa State, Nigeria. *Appl. Water Sci.* **2022**, *12*, 10. [CrossRef]
37. Doke, A.B.; Zolekar, R.B.; Patel, H.; Das, S. Geospatial mapping of groundwater potential zones using multi-criteria decision-making AHP approach in a hardrock basaltic terrain in India. *Ecol. Indic.* **2021**, *127*, 107685. [CrossRef]
38. Allafra, H.; Opp, C.; Patra, S. Identification of groundwater potential zones using remote sensing and GIS techniques: A case study of the shatt Al-Arab Basin. *Remote Sens.* **2021**, *13*, 112. [CrossRef]
39. Benjmel, K.; Amraoui, F.; Boutaleb, S.; Ouchchen, M.; Tahiri, A.; Touab, A. Mapping of groundwater potential zones in crystalline terrain using remote sensing, GIS techniques, and multicriteria data analysis (Case of the ighrem region, Western Anti-Atlas, Morocco). *Water* **2020**, *12*, 471. [CrossRef]
40. Kanagaraj, G.; Suganthi, S.; Elango, L.; Magesh, N.S. Assessment of groundwater potential zones in Vellore district, Tamil Nadu, India using geospatial techniques. *Earth Sci. Inform.* **2019**, *12*, 211–223. [CrossRef]
41. Ajay Kumar, V.; Mondal, N.C.; Ahmed, S. Identification of Groundwater Potential Zones Using RS, GIS and AHP Techniques: A Case Study in a Part of Deccan Volcanic Province (DVP), Maharashtra, India. *J. Indian Soc. Remote Sens.* **2020**, *48*, 497–511. [CrossRef]
42. TOB. Mersin Tarımsal Yatırım Rehberi. Available online: [https://www.tarimorman.gov.tr/SGB/TARYAT/Belgeler/il\\_yatirim\\_rehberleri/mersin.pdf](https://www.tarimorman.gov.tr/SGB/TARYAT/Belgeler/il_yatirim_rehberleri/mersin.pdf) (accessed on 21 February 2022). (In Turkish)
43. TadPortal. Tarım Arazileri Değerlendirme ve Yönetim Otomasyonu. 8 October 2021. Available online: <http://tad.tarim.gov.tr/TadPortal> (accessed on 8 October 2021). (In Turkish)
44. WorldClim. Annual Average Precipitation. Available online: <https://www.worldclim.org/> (accessed on 8 November 2021).
45. ATLAS. ATLAS application. Available online: <https://basic.atlas.gov.tr/> (accessed on 8 November 2021).
46. USGS. World Geologic Maps. Available online: <https://certmapper.cr.usgs.gov/data/apps/world-maps/> (accessed on 8 October 2021).
47. CLMS. Copernicus Land Monitoring Service. 2021. Available online: <https://land.copernicus.eu/> (accessed on 8 July 2021).
48. TÜİK. Turkish Statistical Institute. Available online: <https://data.tuik.gov.tr/Bulten/Index?p=Kent-Kir-Nufus-Istatistikleri-2022-49755> (accessed on 17 May 2023).
49. Orhan, O. Monitoring of land subsidence due to excessive groundwater extraction using small baseline subset technique in Konya, Turkey. *Environ. Monit. Assess.* **2021**, *193*, 174. [CrossRef]
50. General Directorate of Meteorology. Seasonal Normals of the Provinces (İllerin Mevsim Normalleri—In Turkish). Available online: <https://www.mgm.gov.tr/veridegerlendirme/il-ve-ilceler-istatistik.aspx?m=MERSIN> (accessed on 7 April 2021).
51. Weather. The World Average Annual Precipitation. Available online: <https://www.eldoradoweather.com/climate/world-maps/world-annual-precip-map.html> (accessed on 6 July 2021).
52. Ma, H.; Zhu, Q.; Zhao, W. Soil water response to precipitation in different micro-topographies on the semi-arid Loess Plateau, China. *J. For. Res.* **2020**, *31*, 245–256. [CrossRef]
53. Arivalagan, S.; Kiruthika, A.M.; Sureshbabu, S. Delineation of groundwater potential zones using RS and GIS techniques: A case study for Eastern part of Krishnagiri district, Tamil Nadu. *Int. J. Adv. Res. Sci. Eng. Technol.* **2014**, *3*, 51–59.
54. Riihimäki, H.; Kemppinen, J.; Kopecký, M.; Luoto, M. Topographic Wetness Index as a Proxy for Soil Moisture: The Importance of Flow-Routing Algorithm and Grid Resolution. *Water Resour. Res.* **2021**, *57*, e2021WR029871. [CrossRef]
55. Mallick, J.; Khan, R.A.; Ahmed, M.; Alqadhi, S.D.; Alsubih, M.; Falqi, I.; Hasan, M.A. Modeling Groundwater Potential Zone in a Semi-Arid Region of Aseer Using Fuzzy-AHP and Geoinformation Techniques. *Water* **2019**, *11*, 2656. [CrossRef]
56. Rizeei, H.M.; Pradhan, B.; Saharkhiz, M.A.; Lee, S. Groundwater aquifer potential modeling using an ensemble multi-adoptive boosting logistic regression technique. *J. Hydrol.* **2019**, *579*, 124–172. [CrossRef]
57. Shao, Z.; Huq, M.E.; Cai, B.; Altan, O.; Li, Y. Integrated remote sensing and GIS approach using Fuzzy-AHP to delineate and identify groundwater potential zones in semi-arid Shanxi Province, China. *Environ. Model. Softw.* **2020**, *134*, 104868. [CrossRef]

58. Naghibi, S.A.; Moghaddam, D.D.; Kalantar, B.; Pradhan, B.; Kisi, O. A comparative assessment of GIS-based data mining models and a novel ensemble model in groundwater well potential mapping. *J. Hydrol.* **2017**, *548*, 471–483. [[CrossRef](#)]
59. Pinto, D.; Shrestha, S.; Babel, M.S.; Ninsawat, S. Delineation of groundwater potential zones in the Comoro watershed, Timor Leste using GIS, remote sensing and analytic hierarchy process (AHP) technique. *Appl. Water Sci.* **2017**, *7*, 503–519. [[CrossRef](#)]
60. Sitender, R. Delineation of groundwater potential zones in Mewat District, Haryana, India. *Int. J. Geomat. Geosci.* **2010**, *2*, 270–281.
61. Botzen, W.J.W.; Aerts, J.C.J.H.; van den Bergh, J.C.J.M. Individual preferences for reducing flood risk to near zero through elevation. *Mitig. Adapt. Strateg. Glob. Chang.* **2013**, *18*, 229–244. [[CrossRef](#)]
62. Rizeei, H.M.; Pradhan, B.; Saharkhiz, M.A. Surface runoff estimation and prediction regarding LULC and climate dynamics using coupled LTM, optimized arima and distributed-GIS-based SCS-CN models at tropical region. In Proceedings of the Global Civil Engineering Conference, Kuala Lumpur, Malaysia, 25–28 July 2017. [[CrossRef](#)]
63. Vasudevan, S.; Pauline, M.J.; Balamurugan, P.; Sahoo, S.K. Delineation of groundwater potential zones in Coimbatore district, Tamil Nadu, using Remote sensing and GIS techniques. *Int. J. Eng. Res. Gen. Sci.* **2015**, *3*, 203–214.
64. Li, Z.; Fang, H. Impacts of climate change on water erosion: A review. *Earth-Sci. Rev.* **2016**, *163*, 94–117. [[CrossRef](#)]
65. Guo, S.; Zhu, D.Z. Soil and Groundwater Erosion Rates into a Sewer Pipe Crack. *J. Hydraul. Eng.* **2017**, *143*, 1–5. [[CrossRef](#)]
66. Ahmad, I.; Dar, M.A.; Andualem, T.G.; Tekka, A.H. Groundwater development using geographic information system. *Appl. Geomat.* **2020**, *12*, 73–82. [[CrossRef](#)]
67. Hou, E.; Wang, J.; Chen, W. A comparative study on groundwater spring potential analysis based on statistical index, index of entropy and certainty factors models. *Geocarto Int.* **2018**, *33*, 754–769. [[CrossRef](#)]
68. Park, S.; Hamm, S.Y.; Jeon, H.T.; Kim, J. Evaluation of logistic regression and multivariate adaptive regression spline models for groundwater potential mapping using R and GIS. *Sustainability* **2017**, *9*, 1157. [[CrossRef](#)]
69. Zhang, Y.; Shi, P.; Li, F.; Wei, A.; Song, J.; Ma, J. Quantification of nitrate sources and fates in rivers in an irrigated agricultural area using environmental isotopes and a Bayesian isotope mixing model. *Chemosphere* **2018**, *208*, 493–501. [[CrossRef](#)]
70. Yang, Y.; Lian, X.Y.; Jiang, Y.H.; Xi, B.D.; He, X.S. Risk-based prioritization method for the classification of groundwater pesticide pollution from agricultural regions. *Integr. Environ. Assess. Manag.* **2017**, *13*, 1052–1059. [[CrossRef](#)] [[PubMed](#)]
71. Mukherjee, P.; Singh, C.K.; Mukherjee, S. Delineation of Groundwater Potential Zones in Arid Region of India-A Remote Sensing and GIS Approach. *Water Resour. Manag.* **2012**, *26*, 2643–2672. [[CrossRef](#)]
72. Iban, M.C.; Sahin, E. Monitoring Land Use and Land Cover Change Near a Nuclear Power Plant Construction Site: Akkuyu Case. *Environ. Monit. Assess.* **2022**, *194*, 724. [[CrossRef](#)] [[PubMed](#)]
73. Saaty, T.L. *The Analytic Hierarchy Process*; McGraw-Hill: New York, NY, USA, 1980.
74. Orhan, O.; Yakar, M.; Ekerin, S. An application on sinkhole susceptibility mapping by integrating remote sensing and geographic information systems. *Arab. J. Geosci.* **2020**, *13*, 886. [[CrossRef](#)]
75. Saaty, T.L. How to make a decision: The analytic hierarchy process. *Eur. J. Oper. Res.* **1990**, *48*, 9–26. [[CrossRef](#)]
76. Saaty, T.L. Decision making with the Analytic Hierarchy Process. *Int. J. Serv. Sci.* **2008**, *1*, 83–89. [[CrossRef](#)]
77. Yalpir, S.; Sisman, S.; Akar, A.U.; Unel, F.B. Feature selection applications and model validation for mass real estate valuation systems. *Land Use Policy* **2021**, *108*, 105539. [[CrossRef](#)]
78. Saaty, R.W. The analytic hierarchy process—What it is and how it is used. *Math. Model.* **1987**, *9*, 161–176. [[CrossRef](#)]
79. Bilgilioglu, S.S.; Gezgin, C.; Orhan, O.; Karakus, P. A GIS-based multi-criteria decision-making method for the selection of potential municipal solid waste disposal sites in Mersin, Turkey. *Environ. Sci. Pollut. Res.* **2022**, *29*, 5313–5329. [[CrossRef](#)]
80. Salihoglu, T. Delimiting Istanbul's Urban Centers Through GIS. *J. Geomat.* **2020**, *5*, 201–208. [[CrossRef](#)]
81. Opricovic, S.; Tzeng, G.-H. Compromise solution by MCDM methods: A comparative analysis of VIKOR and TOPSIS. *Eur. J. Oper. Res.* **2004**, *156*, 445–455. [[CrossRef](#)]
82. Hwang, C.L.; Yoon, K. Methods for multiple attribute decision making. In *Lecture Notes in Economics and Mathematical Systems*; Springer: Berlin/Heidelberg, Germany, 1981; pp. 58–191. [[CrossRef](#)]
83. Jozaghi, A.; Alizadeh, B.; Hatami, M.; Flood, I.; Khorrami, M.; Khodaei, N.; Ghasemi Tousi, E. A comparative study of the AHP and TOPSIS techniques for dam site selection using GIS: A case study of Sistan and Baluchestan Province. *Geosciences* **2018**, *8*, 494. [[CrossRef](#)]
84. Kuo, T. A modified TOPSIS with a different ranking index. *Eur. J. Oper. Res.* **2017**, *260*, 152–160. [[CrossRef](#)]
85. Wang, Y.; Qiu, M.; Shi, L.; Xu, D.; Liu, T.; Qu, X. A GIS-based model of potential groundwater yield zonation for a sandstone aquifer based on the EWM and TOPSIS methods. In Proceedings of the IMWA 2019 “Mine Water: Technological and Ecological Challenges”, Perm, Russia, 15–19 July 2019; pp. 387–393.
86. Wang, Z.; Wang, J.; Zhang, G.; Wang, Z. Evaluation of agricultural extension service for sustainable agricultural development using a hybrid entropy and TOPSIS method. *Sustainability* **2021**, *13*, 347. [[CrossRef](#)]
87. Mohsin, M.; Zhang, J.; Saidur, R.; Sun, H.; Sait, S.M. Economic assessment and ranking of wind power potential using fuzzy-TOPSIS approach. *Environ. Sci. Pollut. Res.* **2019**, *26*, 22494–22511. [[CrossRef](#)]
88. Chen, W.; Panahi, M.; Khosravi, K.; Pourghasemi, H.R.; Rezaie, F.; Parvinnezhad, D. Spatial Prediction of Groundwater Potentiality Using ANFIS Ensembled with Teaching-learning-based and Biogeography-based Optimization. *J. Hydrol.* **2019**, *572*, 435–448. [[CrossRef](#)]

89. Naghibi, S.A.; Pourghasemi, H.R.; Dixon, B. GIS-based Groundwater Potential Mapping Using Boosted Regression Tree, Classification and Regression Tree, and Random Forest Machine Learning Models in Iran. *Environ. Monit. Assess.* **2016**, *188*, 44. [[CrossRef](#)]
90. Guru, B.; Seshan, K.; Bera, S. Frequency Ratio Model for Groundwater Potential Mapping and Its Sustainable Management in Cold Desert, India. *J. King Saud Univ.-Sci.* **2017**, *29*, 333–347. [[CrossRef](#)]
91. Prasad, P.; Loveson, V.J.; Kotha, M.; Yadav, R. Application of machine learning techniques in groundwater potential mapping along the west coast of India. *GIScience Remote Sens.* **2020**, *57*, 735–752. [[CrossRef](#)]
92. Upwanshi, M.; Damry, K.; Pathak, D.; Tikle, S.; Das, S. Delineation of potential groundwater recharge zones using remote sensing, GIS, and AHP approaches. *Urban Clim.* **2023**, *48*, 101415. [[CrossRef](#)]
93. Golkarian, A.; Naghibi, S.A.; Kalantar, B.; Pradhan, B. Groundwater Potential Mapping Using C5.0, Random Forest, and Multivariate Adaptive Regression Spline Models in GIS. *Environ. Monit. Assess.* **2018**, *190*, 149. [[CrossRef](#)]
94. Pradhan, B.; Lee, S. Delineation of landslide hazard areas on Penang Island, Malaysia, by using frequency ratio, logistic regression, and artificial neural network models. *Environ. Earth Sci.* **2010**, *60*, 1037–1054. [[CrossRef](#)]
95. Ha, D.H.; Nguyen, P.T.; Costache, R.; Al-Ansari, N.; Phung, T.V.; Nguyen, D.; Amiri, M.; Prakash, I.; Le, H.V.; Nguyen, H.B.; et al. Quadratic Discriminant Analysis Based Ensemble Machine Learning Models for Groundwater Potential Modeling and Mapping. *Water Resour. Manag.* **2021**, *35*, 4415–4433. [[CrossRef](#)]
96. Ghosh, D.; Mandal, M.; Karmakar, M.; Banarjee, M.; Mandal, D. Application of geospatial technology for delineating groundwater potential zones in the Gandheswari watershed, West Bengal. *Sustain. Water Resour. Manag.* **2020**, *6*, 14. [[CrossRef](#)]
97. Nsiah, E.; Appiah-Adjei, E.K.; Adjei, K.A. Hydrogeological delineation of groundwater potential zones in the Nabogo basin, Ghana. *J. Afr. Earth Sci.* **2018**, *143*, 1–9. [[CrossRef](#)]
98. Sikdar, P.K.; Chakraborty, S.; Adhya, E.; Paul, P.K. Land Use/Land Cover Changes and Groundwater Potential Zoning in and around Raniganj coal mining area, Bardhaman District, West Bengal—A GIS and Remote Sensing Approach. *J. Spat. Hydrol.* **2004**, *4*, 5.
99. Sajil Kumar, P.J.; Elango, L.; Schneider, M. GIS and AHP Based Groundwater Potential Zones Delineation in Chennai River Basin (CRB), India. *Sustainability* **2022**, *14*, 1830. [[CrossRef](#)]
100. Zhu, Q.; Abdelkareem, M. Mapping groundwater potential zones using a knowledge-driven approach and GIS analysis. *Water* **2021**, *13*, 579. [[CrossRef](#)]
101. Yilmaz, C.B.; Demir, V.; Sevimli, M.F.; Demir, F.; Yakar, M. Trend analysis of temperature and Precipitation in Mediterranean region. *AGIS* **2021**, *1*, 15–21.
102. Pradhan, A.M.S.; Kim, Y.T.; Shrestha, S.; Huynh, T.C.; Nguyen, B.P. Application of deep neural network to capture groundwater potential zone in mountainous terrain, Nepal Himalaya. *Environ. Sci. Pollut. Res.* **2021**, *28*, 18501–18517. [[CrossRef](#)] [[PubMed](#)]
103. Srivastava, P.K.; Bhattacharya, A.K. Groundwater assessment through an integrated approach using remote sensing, GIS and resistivity techniques: A case study from a hard rock terrain. *Int. J. Remote Sens.* **2006**, *27*, 4599–4620. [[CrossRef](#)]
104. Brito, T.P.; Bacellar, L.A.; Barbosa, M.S.C.; Barella, C.F. Assessment of the groundwater favorability of fractured aquifers from the southeastern Brazil crystalline basement. *Hydrol. Sci. J.* **2020**, *65*, 442–454. [[CrossRef](#)]
105. Kim, Y.; Chung, E.S. Robust prioritization of climate change adaptation strategies using the VIKOR method with objective weights. *JAWRA J. Am. Water Resour. Assoc.* **2015**, *51*, 1167–1182. [[CrossRef](#)]
106. Chang, C.L.; Hsu, C.H. Applying a Modified VIKOR Method to Classify Land Subdivisions According to Watershed Vulnerability. *Water Resour. Manag.* **2011**, *25*, 301–309. [[CrossRef](#)]
107. Njock, P.G.A.; Shen, S.L.; Zhou, A.; Lin, S.S. A VIKOR-based approach to evaluate river contamination risks caused by wastewater treatment plant discharges. *Water Res.* **2022**, *226*, 119288. [[CrossRef](#)]
108. Özer, O. Modelling and Determination of Groundwater Pollution and an Investigation of Pollutant Sources Using Isotope Methods, Establishing Geographic Information Systems in the Göksu Delta. Ph.D. Thesis, Mersin University, Mersin, Turkey, 2014.
109. Yuka, F. Groundwater Quality Evaluation of Tarsus Coastal Aquifer (Mersin) Using Geographical Information Systems and Water Quality Indices. Master's Thesis, Mersin University, Mersin, Turkey, 2021.
110. Dalçık, A. Determination of the Groundwater Potential of Akdere-Yeşilovacik (Silifke, Mersin) Region by Geographical Information System and Analytical Hierarchy Process Methods. Master's Thesis, Mersin University, Mersin, Turkey, 2022.
111. Cetin, M. The changing of important factors in the landscape planning occur due to global climate change in temperature, Rain and climate types: A case study of Mersin City. *Turk. J. Agric. Food Sci. Technol.* **2020**, *8*, 2695–2701. [[CrossRef](#)]
112. Celiker, S.; Sarac Essiz, E.; Oturakci, M. Integrated Ahp-Fmea Risk Assessment Method To Stainless Tank Production Process. *Turk. J. Eng.* **2021**, *5*, 118–122. [[CrossRef](#)]
113. Rahman, M.M.; AlThobiani, F.; Shahid, S.; Viridis, S.G.P.; Kamruzzaman, M.; Rahaman, H.; Momin, M.A.; Hossain, M.B.; Ghandourah, E.I. GIS and remote sensing-based multi-criteria analysis for delineation of groundwater potential zones: A case study for industrial zones in Bangladesh. *Sustainability* **2022**, *14*, 6667. [[CrossRef](#)]
114. Nga, D.V.; Trang, P.T.K.; Duyen, V.T.; Mai, T.T.; Lan, V.T.M.; Viet, P.H.; Postma, D.; Jakobsen, R. Spatial variations of arsenic in groundwater from a transect in the Northwestern Hanoi. *Vietnam. J. Earth Sci.* **2017**, *40*, 70–77. [[CrossRef](#)]
115. El-Mezayen, M.M.; El-Hamid, A.; Hazem, T. Assessment of Water Quality and Modeling Trophic Level of Lake Manzala, Egypt Using Remotely Sensed Observations after Recent Enhancement Project. *J. Indian Soc. Remote Sens.* **2023**, *51*, 197–211. [[CrossRef](#)]

116. Jannat, J.N.; Khan, M.S.I.; Islam, H.M.T.; Islam, M.S.; Khan, R.; Siddique, M.A.B.; Varol, M.; Tokatli, C.; Pal, S.C.; Islam, A.; et al. Hydro-chemical assessment of fluoride and nitrate in groundwater from east and west coasts of Bangladesh and India. *J. Clean. Prod.* **2022**, *372*, 133675. [[CrossRef](#)]
117. Priya, U.; Iqbal, M.A.; Salam, M.A.; Nur-E-Alam, M.; Uddin, M.F.; Islam, A.R.M.T.; Sarkar, S.K.; Imran, S.S.; Rak, A.E. Sustainable groundwater potential zoning with integrating GIS, remote sensing, and AHP model: A case from North-Central Bangladesh. *Sustainability* **2022**, *14*, 5640. [[CrossRef](#)]

**Disclaimer/Publisher's Note:** The statements, opinions and data contained in all publications are solely those of the individual author(s) and contributor(s) and not of MDPI and/or the editor(s). MDPI and/or the editor(s) disclaim responsibility for any injury to people or property resulting from any ideas, methods, instructions or products referred to in the content.